



Universiteit
Utrecht

*Improving Stability of Palladium Nitrate
Precursor Solutions by Fuming Nitric Acid
Recrystallization Towards Efficient
Bimetallic Ni-Pd/SiO₂ Catalysts for
Hydrogenation reactions*

Master Thesis

Group of Inorganic Chemistry and Catalysis

Debye Institute for Nanomaterials Science

Utrecht University

V.P.J. (Vincent) de Vries, BSc

Student number: 4277864

Period of the project: '20-'21

Daily supervisor: F. (Florian) Zand, MSc

MSc Project supervisor: dr. W. (Ward) van der Stam

Second examiner: dr. F. (Florian) Meirer

I Abstract

Bimetallic systems in catalysts could lead to enhanced catalysis resulting in milder reaction conditions and higher turnover rate. The monometallic Nickel on Silica oxide catalysts is often used for hydrogenation reactions, but has limited activity at low temperature. Adding a noble metal in the form of Palladium could enhance the catalyst leading to a bimetallic alloy favorable to certain hydrogenation reactions such as CO₂ methanation. Yet, addition of Palladium does not result directly into an improved bimetallic system over the monometallic Nickel catalyst as most of the Palladium in monometallic system is on the outside of the support caused by large sintering. Here we show that recrystallization of the Palladium nitrate source, containing Palladium oxide particles, by using fuming nitric acid as a recrystallization agent leads to enhanced stability of the precursor solution. During synthesis of Palladium catalysts different Palladium nitrate sources were used containing large differences in purity. As a result, the optimal precursor conditions leading to the most active and stable catalyst were not affected by the acidity of the solution but by the fast sintering of Palladium (oxide) particles. These results show that recrystallizing Palladium nitrate sources by fuming nitric acid and vacuum evaporation leads to a general form of Palladium nitrate consisting of little to no Palladium oxide. By repeating the recrystallization with fuming nitric acid ultimately could lead to pure Palladium nitrate sources and enhanced stability of precursor conditions showing no sign of particle formation. Most of the Palladium metal can then enter the support leading to Nickel-Palladium alloying and optimal ratio and weight percentage of metal can be characterized improving the catalyst performance making large CO₂ emissions useful for reusage.

II List of abbreviations

When no units are indicated the abbreviation is unitless or just an abbreviation.

τ	Mean size of crystalline domains (nm)
θ	X-ray incidence angle, also called Bragg Angle (°)
Θ	Contact angle between liquid and solid surface (°)
γ	Surface tension (J/m ²)
λ_0	Wavelength of the X-ray (nm)
β	Line broadening at half the maximum intensity (FWHM)
ΔH_{298}	Enthalpy at 298K
A	Absorbance (a.u.)
Abs	Absorbance (a.u.)
b	Path length (cm)
c	Concentration (mol/L)
d	Lattice spacing of a crystal (nm)
DI	Dry Impregnation, same as IWI
DRIFTS	Diffuse Reflectance Infrared Fourier Transform Spectroscopy
ϵ	Molar absorptivity (L/mol/cm)
FWHM	Full Width at Half Maximum (nm)
GHSV	Gas Hourly Space Velocity (h ⁻¹)
HLLW	High Level Liquid Waste
I	Non absorbed light
I_0	Light emitted by the light source
ICP-OES	Inductively Coupled Plasma Optical Emission Spectroscopy
IEP	Iso-Electric Point

IWI	Incipient Wetness Impregnation
K	Shape factor
LMCT	Ligand to Metal Charge Transfer
M	Molarity (mol/L)
M...	Molar mass (g/mol)*
m	Mass (g)
MLCT	Metal to Ligand Charge Transfer
ρ	Density (g/ml)
P	Capillary pressure (kg/m ²)
r	Pore radius (m)
TCD	Thermal Conductivity Reactor
TEM	Transmission Electron Microscopy
TOF	Turnover Frequency (mol product/s/mol metal)
TPR	Temperature Programmed Reduction
UV-vis	Ultra-Violet and visible light
V	Volume (ml)
XRD	X-Ray Diffraction
ZPC	Zero Point of Charge, same as IEP

* ... Indicates that the abbreviation must have an indication on which subject it holds, otherwise a different abbreviation is used.

Contents

I ABSTRACT	- 3 -
II LIST OF ABBREVIATIONS.....	- 4 -
1. INTRODUCTION	- 8 -
2. THEORY	- 11 -
2.1 SYNTHESIZING CATALYSTS	- 11 -
2.1.1 <i>Incipient wetness impregnation</i>	- 11 -
2.1.2 <i>Support and precursor solution</i>	- 12 -
2.1.3 <i>Drying of the impregnated support</i>	- 14 -
2.1.4 <i>Calcination of the dried support</i>	- 14 -
2.1.5 <i>Reduction of calcined catalysts</i>	- 15 -
2.2 PALLADIUM NITRATE FOR PRECURSOR SOLUTION	- 16 -
2.3 NITRIC ACID	- 17 -
2.4 CHARACTERIZATION TECHNIQUES.....	- 18 -
2.4.1 <i>UV-Vis spectroscopy</i>	- 18 -
2.5.2 <i>X-ray diffraction</i>	- 21 -
2.5.3 <i>Catalytic testing on operando system</i>	- 22 -
3. EXPERIMENTAL.....	- 23 -
3.1 CHEMICALS.....	- 23 -
3.2 SYNTHESIZING (FUMING) NITRIC ACID	- 23 -
3.3 RECRYSTALLIZATION OF PALLADIUM NITRATE	- 25 -
3.3.1 <i>Using fuming nitric acid</i>	- 25 -
3.3.2 <i>Vacuum drying</i>	- 25 -
3.3.3 <i>Using concentrated nitric acid</i>	- 26 -
3.4 SYNTHESIZING PALLADIUM ON SiO ₂ CATALYSTS	- 26 -
3.4.1 <i>Impregnation of precursor solution on support</i>	- 27 -
3.4.2 <i>Calcination and reduction of impregnated support</i>	- 27 -

3.5 CHARACTERIZATION TECHNIQUES	- 27 -
3.5.1 UV-vis.....	- 27 -
3.5.2 XRD	- 28 -
3.5.3 Catalytic testing.....	- 29 -
4. RESULTS AND DISCUSSION	- 30 -
4.1 SYNTHESIZING FUMING NITRIC ACID	- 31 -
4.2 RECRYSTALLIZATION OF PALLADIUM NITRATE HYDRATE	- 32 -
4.2 ICP-OES.....	- 34 -
4.3 UV-VIS	- 36 -
4.3.1 Stability (old) 39% Palladium nitrate.....	- 38 -
4.3.2 Stability (new) 41% Palladium nitrate	- 40 -
4.3.3 Stability recrystallized Palladium nitrate.....	- 41 -
4.3.4 BIMETALLIC PRECURSOR STABILITY	- 44 -
4.5 TRANSMISSION ELECTRON MICROSCOPY	- 46 -
4.6 X-RAY DIFFRACTION.....	- 50 -
4.7 OPERANDO INFRARED RADIATION.....	- 55 -
5. CONCLUSION	- 59 -
6. OUTLOOK	- 62 -
7. ACKNOWLEDGEMENTS.....	- 66 -
8. BIBLIOGRAPHY	- 67 -
9. APPENDIX.....	- 74 -

1. Introduction

Recently, there has been a strong debate about global warming. Consequences of this are for instance extreme weather; tropical cyclones are getting more common, faster, stronger and larger due to warmer climates. [1]. Studies show that humans caused an increase of at least 1,5°C. [2] Globally, the 10 hottest years happened all in this century, with 2019 the second warmest year ever recorded (2020 not included). [3] Most important effect of global warming is the non-reversible melting of the ice caps, resulting in a fast increase of the sea-level. [4] One of the causes of global warming can be attributed to the exponentially increased CO₂ levels in the air over the last decades, see figure 1a. [5] CO₂ is a gas that, together with N₂O and CH₄, can hold heat from the sun easily, [6] by absorbing infrared radiation that is normally scattered back into space. [7]

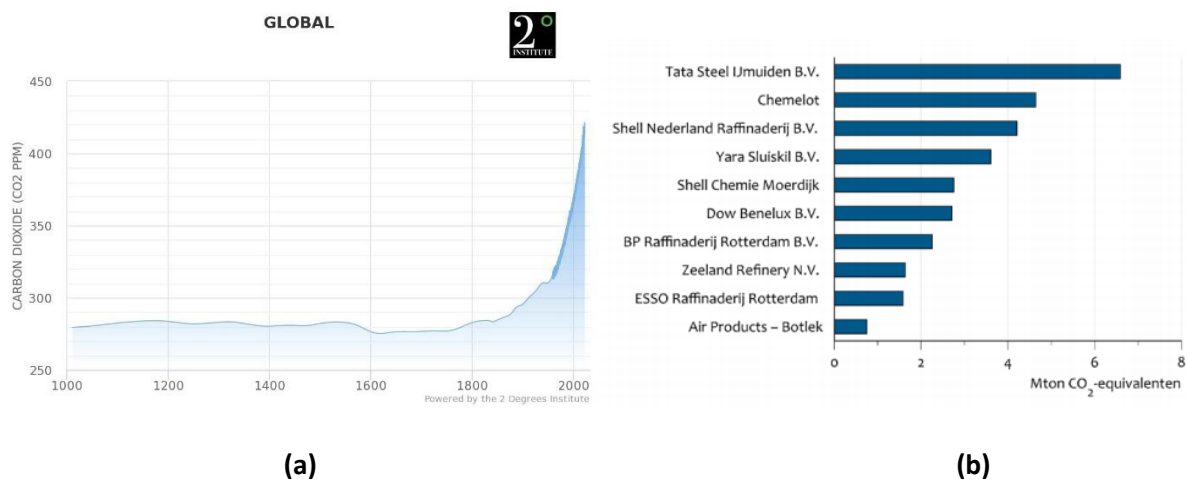


Figure 1. **a** Global CO₂ levels from 1000-2021, adapted from [5]. **b** Top 10 CO₂ emission in megatons from industries in the Netherlands in 2018, adapted from [8].

In figure 1b the top 10 larger CO₂ emitters in the Netherlands are given. [9] In total 20% of all the CO₂ is emitted by industries in the Netherlands in 2020. [10] When this amount of CO₂ emittance can be reduced, a large step is made into a more durable future and reaching the values decided in the Paris

agreement. [11] Smart catalysts are needed for large scale CO₂ recycling and reuse directly from industries for new products.

The functioning of catalysts was found in 1817 by Sir Humphrey Davy. [12] [13] Since then, progress is made and new discoveries are found in this emerging field leading towards catalysts used today. [14] When a heterogeneous catalyst is used, recognizable to the deviating phase of the catalyst to the reacting molecules, less energy is needed to perform certain reactions due to a more reachable intermediate phase transformation. [15] It was observed that smaller particles (or even nanoparticles) had different magnetic and electronic properties as bulk material, due to certain size effects induced by the high surface to volume ratio. [16] These effects are induced from pore sizes and properties of supports [17] leading to size selective catalysts, useful to require or prevent certain compounds. [18]

One of the most interesting fields to discover are bimetallic catalysts. In the right conditions, bimetallic catalysts create a structure that enhances stability, selectivity and activity towards the favorable reaction, being the most important aspects of catalysis. [19] The bimetallic structure, containing the right ratio of metals in alloy, will determine the working of the catalyst. Moreover, core shelled formation conducts rise and can benefit a reaction. [14] [20] For this research it is important to find the optimal ratio between the two metals, resulting in high affinity towards certain reactions.

Currently, nickel-based catalysts are the most widely studied supported catalyst. [21] Supported nickel is used in CO₂ hydrogenation catalysts because of its ability to split CO bonds and its high hydrogenation activity. [22] Nickel's limitations are the operating conditions: at temperatures below 300°C nickel will deactivate in oxidation to Ni(CO)₄. [23] As CO₂ methanation is favored at low temperatures of 250-500°C, [24] the catalyst should be stable during these conditions. To make the catalyst more stable at milder reaction conditions a second metal leads to some favorable abilities towards the several aspects of the catalyst such as lower transition states.

An efficient option for an active phase in a bimetallic catalyst are noble metals, such as Platinum and Rhodium, as they lead to high selectivity towards methane. [21] Downside is that they are more expensive than non-noble metals, in most cases. Palladium, as a noble metal, would be useful as the price is significantly lower than Ruthenium and other noble metals. [20] Besides the different metal, it is known from studies that depending the metal oxide of a support different products would be favorable, such as Palladium on Silica oxide support would favor methanol formation on several reactants. [25] Yet, the interaction between Palladium compounds and the (Silica) support is relatively weak and severe sintering of large metal clusters occurs. [26] Moreover, sintering of Palladium can have several causes and this is one important subject of this thesis and is analyzed how the formation of large Palladium 'chunks' outside the support can be prevented.

The subject of this thesis is on describing and analyzing the issues and behavior (i.e. formation of PdO) in solution of different Palladium species in catalysts as well in precursor form. This will lead to enhanced stability towards the most stable Palladium species that makes defined catalysts. The knowledge gained here is an excellent start towards synthesizing active catalysts with an optimal ratio between Nickel (or other metal) and Palladium which can be different depending on the reaction and conditions used during catalytic testing.

The Palladium source used is Palladium nitrate, which is not completely pure and will be recrystallized to increase the purity. This will be done with recrystallization agent fuming nitric acid, which was made from reaction of Potassium nitrate and sulfuric acid and distilled, as well as with concentrated (68%) nitric acid. As a result, the amount of Palladium in the salt form is increased and the amount of Palladium oxide is decreased. To obtain a feeling for the purity, the purity is measured with ICP-OES as well as with X-ray Diffraction (XRD). The stability (if the solution forms Palladium oxide) in different concentrations of nitric acid is tested with UV-vis spectroscopy. Further, the more stable precursor solution is compared with the original precursor solution synthesized to a catalyst, see figure 2. The particle size of the Palladium (oxide) nanoparticles are measured with X-ray Diffraction and the sintering outside the support was measured with electron microscopy. The thesis ended with examining bimetallic precursor solutions of Nickel nitrate and Palladium nitrate (not pure) for future synthesis of bimetallic catalysts. The optimal concentration of nitric acid is analyzed.

The recrystallization resulted in significant purer Palladium nitrate, which resulted in a more stable precursor solution. The fuming nitric acid, as expected, worked better than the concentrated nitric in purity as well as stability. As a result, the metal particle size in Silica oxide support was overall smaller, but this had no significant influence on the activity. It was unclear if the purer Palladium nitrate resulted in less sintering.

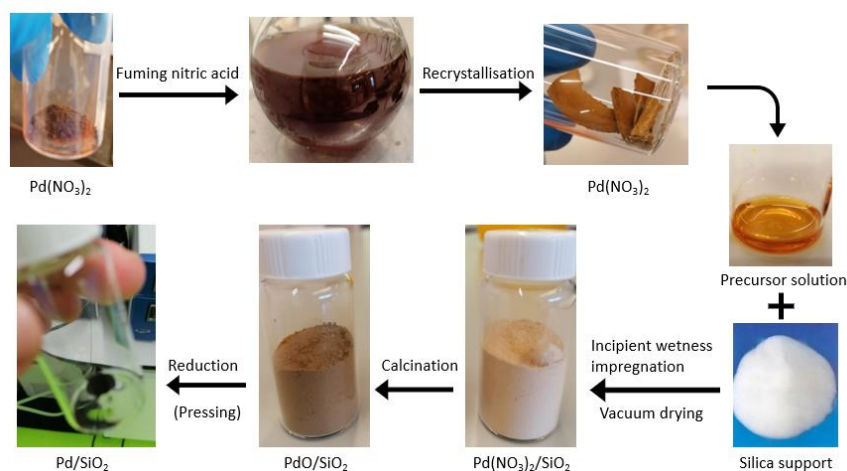


Figure 2. Steps involved in the preparation of Pd/SiO₂ catalysts discussed in this thesis.

2. Theory

As reported in the introduction, the activity of the catalyst depends on the way the catalyst is synthesized. Especially, when using noble metals such as Palladium, which is easily sintered. The preferential qualities of these metals makes it worth finding the best conditions to use them. Studies show that Palladium will make the catalyst more active towards Carbon dioxide methanation by facilitating the dissociative adsorption of Hydrogen and the formation of CO. [22] In a study of Bion et al the working of noble metals on CO oxidation are compared. [27] Bion et al found low activity as well as selectivity for Palladium on different supported catalysts for CO. On cesium supports at high temperature Palladium absorbs more hydrogen than CO molecules, but absorbed hydrogen has more chance to obtain oxidized than CO. [28] On aluminum support different results are found, showing that the support is a huge influencer on the working of the catalyst. The same can be said about using different Palladium sources.

2.1 Synthesizing catalysts

2.1.1 Incipient wetness impregnation

The method that is used for synthesizing catalysts is called dry impregnation (DI) or better known as the incipient wetness impregnation (IWI). [14] On the contrary of wet impregnation, where more precursor solution is used than the total pore volume, for dry impregnation the exact amount of precursor solution as the total volume in the pores is used. Often, the pore volume is known by the producer of the support. The exact volume of a porous support can be measured with Nitrogen physisorption and differential scanning calorimetry. [29] [30] In this section all the different aspects are described that are important for synthesizing catalysts by impregnation, see figure 4.

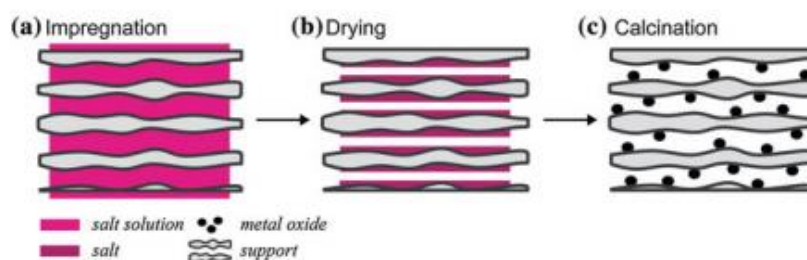


Figure 4. Representation of supported nanoparticle preparation by impregnation and drying. **a** support is loaded with a precursor solution containing the metal as a salt, **b** by drying the solvent is removed and a salt deposit is left inside the pores and **c** after calcination the metal salt is decomposed into a metal oxide and reduced into metal nanoparticles. Adapted from [31].

2.1.2 Support and precursor solution

Supports influence the behavior and formation of nanoparticles. On Cesium oxide supports, for instance, at high temperature Palladium absorbs more hydrogen than CO molecules, but absorbed hydrogen has more chance to obtain oxidized than CO. [28] Cesium oxide supports has a neutral isoelectric point (IEP) of around 7, therefore adsorbing cationic as well as anionic metal salts. The silica support has an acidic character, at a point of zero charge (ZPC) at pH of 1-2, due to the hydroxyl groups. [32] Therefore, cations are often chosen for absorption on the surface. In this case, cations in the form of Palladium tetramine nitrate are not sufficient, but Palladium nitrate could work. Anionic complexes such as Palladium tetrachloride are not useful for impregnation but could be used for supports with a basic character such as Aluminum. [33] Silica supports are used for the lack of acid sites that could contribute to catalytic activity. Therefore, catalytic activity from only the metal particles is measured, without any influence of certain characteristics of the support such as (Lewis) acid sites.

The pore size has a large influence on the size of the particles, see figure 5. When large particles are wanted and the pore size is small the particles could occupy and block the pores, which makes the catalyst inactive as the reactants and/or products can't reach/leave the catalyst.

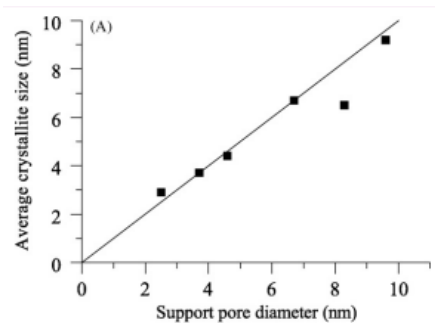


Figure 5. Average crystallite size for Nickel hydroxy nitrate after impregnation and drying at 120°C on silica support at different pore diameters. Adapted from [34].

Secondly, wetting of the precursor solution on the support must be sufficient to induce capillary forces to enter the precursor solution into the pores. If there is sufficient wetting on the support capillary forces are operative and induce pore filling. According to the Laplace-Young equation the capillary pressure can be calculated, see equation 1. [14] For mesoporous hydrophilic supports, that have pore diameters of 2-50 nm, the capillary force are sufficient for wetting when Θ is smaller than 90°. Hydrophobic supports, such as carbon, have a contact angle of larger than 90° which results in a negative capillary pressure. Therefore, extra force or pressure is needed to impregnate the support with a precursor solution.

Equation 1:
$$P = \frac{2\gamma \cos(\theta)}{r}$$

Equation 1. Capillary pressure according to the Laplace-Young equation, where γ is the surface tension of the solution, θ the contact angle between liquid and solid surface and r is the pore radius.

Silica oxide support have a hydrophilic character which shows in infrared (IR) spectra a sharp peak at 3740 cm^{-1} due to isolated hydroxyls and a broader peak at lower wavenumbers raised from hydroxyl groups exhibiting hydrogen bonding. [32] A less polar solvent than water is preferred for a hydrophilic support, due to the surface tension of the solution. Metals will dissolve less well in less polar solutions such as propanol. Impregnating the support in static vacuum could solve this problem, which increases the capillary pressure as the precursor solution is sucked into the pores.

In this thesis there are two different silica supports used. The first one is a support from CARIACT which has a pore volume of 1 ml/g and pore sizes of 10 nm. [35] The other support, from BASF, contained a pore volume of 0.7 ml/g from Nitrogen physisorption, where in theory a maximum of 0.75 ml/g can be reached. [36] Therefore, to reach the same concentration of metal loading on the support, a higher concentration of metal in the precursor solution is needed for the BASF support. A higher metal concentration in precursor solution can have some disadvantages for the catalyst, as some metal salts

are difficult to dissolve completely. If a metal source with low metal percentage is used, it would not even be possible to reach the concentration necessary to have sufficient distribution of metal on the support. Also, higher concentration of metal in precursor solution could lead to higher change of sintering, which leads to loss of surface area. [14]

The CARIACT silica was mainly used on the bimetallic Ni-Pd/SiO₂ catalyst and BASF mainly for experiments on Pd/SiO₂ catalysts. The largest difference is the amount of metal in the precursor solution necessary, as 1.4 times the amount of metal for BASF as for CARIACT is needed, which will make the consistency and stability of the precursor solution more important as the concentration is largest. Although tests on precursor solutions are mainly done with a maximum amount of 5 wt% of metal instead of 7.14 wt%, which could lead to different results.

2.1.3 Drying of the impregnated support

After impregnation the support needs to be dried to remove solution and induce salt deposit on the support. Drying can be done by several techniques and under different conditions. The simplest technique is using heat. By heating up the impregnated support the dissolving liquid is evaporated, and the metals stay behind. Evaporating the liquid by heat from the support could lead to unwanted formation of metal oxide.

Other method for drying, which is mostly used nowadays, is vacuum drying. Benefit is that it is performed at room temperature or even lower temperatures and therefore the metal-nitrate is not yet reacted into metal oxide. The last common method is reasonably new and is called freeze drying. Here, the catalyst is cooled down to low temperatures with liquid nitrogen and then dried at constant temperature of -55°C with vacuum. [37]

The scope of this thesis is on the precursor solution and the result of this precursor solution in the final catalyst. Therefore, vacuum drying was used as it has the smallest influence on the salt impregnated.

2.1.4 Calcination of the dried support

After drying, the metal salt is decomposed into the respective metal oxide, this thermal treatment is called calcination. Thermal programs, which can differ in composition of the gasses, depending on the result wanted. Another reason for calcination is the prevention of formation of unwanted forms during catalytic testing. Different conditions give rise to the way metal oxide particles are distributed over the support, as well as the size of the particles, see figure 5. The temperature program depends on the

temperature that is necessary to decompose the used salt. Generally, only the needed maximum temperature is used to prevent further decomposition of the metal oxide. After calcination, the catalyst is stable to store for some time.

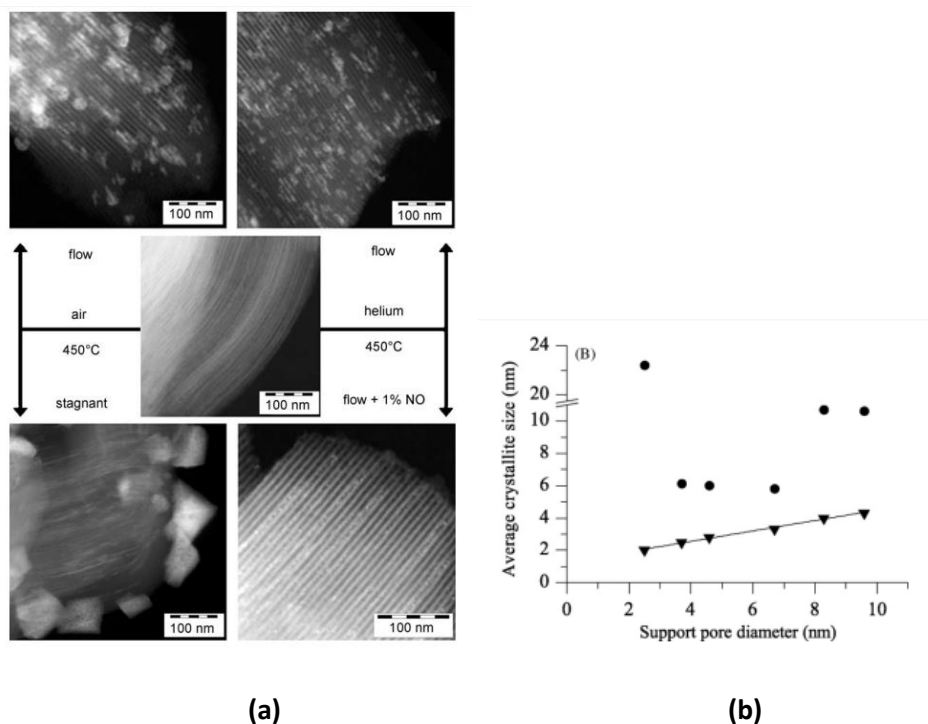
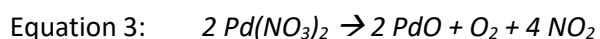
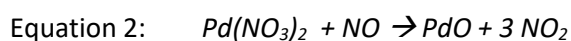


Figure 5. **a** Influence of different calcination conditions on Nickel nitrate supported mesoporous Silica oxide. In white is Nickel oxide and in grey the support. Adapted from [38] **b** The average crystalline size of Nickel oxide obtained after calcination in 1% NO (▼) and in air calcination (●), adapted from [39].

As is visible in figure 5a, using NO will lead to better dispersed particles than only using inert gas. Therefore, in this thesis 10% NO in N₂ is used. The NO gas reacts with the oxygen radicals, preventing the formation of the oxygen molecule, see equation 2 and equation 3. As a result, the decomposition temperature for the metal salt is lower and prevents redistribution of metal salts. Typical color of a calcined palladium catalyst is dark brown.



2.1.5 Reduction of calcined catalysts

The last step in the synthesis of catalysts is the activation of the catalyst. The metal oxide is converted into lone metal particles under hydrogen in an inert atmosphere, see equation 4. The typical color of

a reduced palladium catalyst is black. Depending on the temperature that is needed to convert PdO that temperature can be used. The optimal temperature for a certain catalyst can be found by Temperature Programmed Reduction (TPR). Conditions that are used are 50% H₂/N₂.



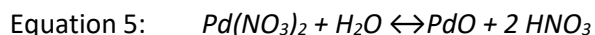
2.2 Palladium nitrate for precursor solution

When it comes to Palladium in catalysts, there are many available salts for precursor solutions. During the research about Palladium catalysts, the most used sources for palladium precursors are Palladium chlorides, Palladium (amine) acetate and Palladium amine nitrates. Studies are done to compare the influence of these different Palladium precursors on the activity of certain hydrogenation reactions. [40] Acetates show reasonable metal dispersion, using amine-chlorides leads to lower dispersion and using chlorides leads to reduced catalysts containing chlorided Palladium types. [41] To prevent the catalyst having chlorides or having acid groups left after reaction, it is best to use a Palladium source that dissolves well. Therefore, it must be possible to remove the cation during the different steps such as drying or calcination. Otherwise, the leftover salt could also inhibit and deactivate the catalyst.

Taking this into account, a logical choice is Palladium nitrates, as nitrates dissolve well in most solvents. Available are Palladium amine nitrates and Palladium nitrates. Palladium amine nitrates contain amines that are in fact reducing agents. [41] But, one of the downsides of using amines is that this compound is only available in a liquid form, which makes it difficult to obtain the right conditions for impregnation. The concentration of Pd²⁺ ions, at 10%, is already low and is dissolved in water. Consequently, the most logical choice is using solid palladium nitrate salts. The benefit is that the concentration of Palladium in the Pd(NO₃)₂·xH₂O complex is around 40% and the salt is in a solid state. Moreover, studies showed reasonable higher activity toward CO hydrogenation for Palladium nitrate precursor solutions as for dinitrodiammine Palladium. [42] Other study showed that the type of Palladium precursor did not had major effects on certain products of Palladium on Silica oxide catalysts. [43] The challenge is to obtain the palladium nitrate salt in a stable composition to create reliable and useful catalysts. At the optimal pH this could lead to stable precursor solutions.

One of the important subjects discussed in the field of HLLW is the pH dependency of Palladium nitrate. Depending on the pH the coordination of the Palladium nitrate molecule in nitric acid solution is different, see figure 6. Different coordination of Palladium nitrate leads to a difference in stability of the molecule, this has several causes. One of the major causes comes from the stability in the reaction

of formation of Palladium oxide. The higher the concentration of water in a solution the more the reaction is onto PdO, see equation 5.



At high pH (pH>0.2), concentration of HNO₃ <0.6M, the [Pd(H₂O)₄]²⁺ is the dominant complex. The [Pd(NO₃)(H₂O)₃]⁺ complex has a maximum at 1.2M HNO₃ and the concentration of the neutral complex Pd(NO₃)₂(H₂O)₂ as well as the [Pd(NO₃)₃(H₂O)]⁻ increases at increasing [HNO₃].

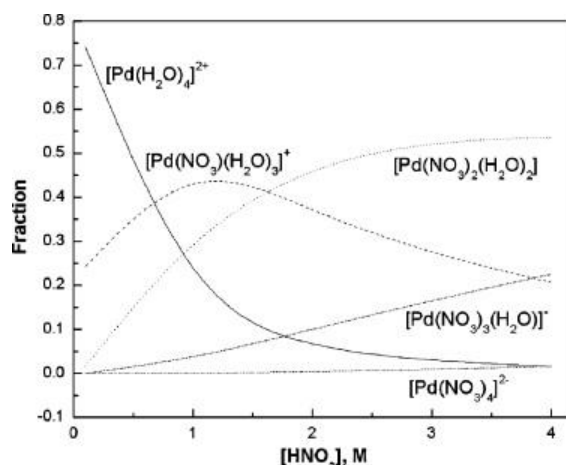


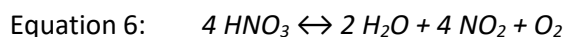
Figure 6. Behavior of Pd(II) nitrate complex in different concentrations of nitric acid, adapted from [44].

In between the concentrations of HNO₃ shown in figure 3, the pK_a value of these Palladium ions is measured at 2.3. [32] At higher pH (pH >1) polynuclear forms are formed, leading to particles of 1.8 nm. Toebes et al concluded that these findings could be interesting for the preparation of Palladium particle sizes in supported catalysts. [32] If a useful way is not found at low pH, maybe using basic conditions could lead to well defined catalysts. Making an alloyed bimetallic catalyst from this could be more difficult.

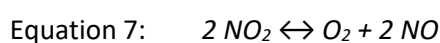
2.3 Nitric acid

One other important component, in this thesis, next to Palladium nitrate is the recrystallization agent nitric acid. As a result of Palladium nitrate degradation in water, see equation 5, nitric acid is formed. As this reaction is in equilibrium the reaction can be pushed towards the Palladium nitrate side, decreasing the amount of PdO in the solution. Moreover, even solid Palladium metal can be dissolved in nitric acid, making Palladium nitrate solution. Being a component in equilibrium makes nitric acid a

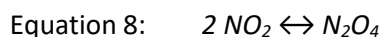
key component in purification of Palladium nitrate salts, which could result in less (or slower) formation of PdO. Not only Palladium nitrate has an equilibrium in solution, nitric acid has an equilibrium even in pure form, see equation 6. [45] This is one of the reasons that pure nitric acid solution is not a common product to buy, yet it is available in the form of 98% purity.



Under exposure of light or heat, nitric acid produces gases and water. Some of these gases stay dissolved in solution, other (part of the) gasses are emitted from the solution when the saturation level is reached. [46] [47] The oxygen and nitrogen dioxide dissolved in solution are in equilibrium with each other, see equation 7. [45] Therefore, nitrous oxide, nitric oxide and oxygen are dissolved in nitric acid.



Dissolved nitrous oxide gives the solution a distinct yellow color, when also nitrogen trioxide is formed the solution turns orange/red, see equation 8. [45] From this color comes the name red fuming nitric acid. Above 86% of purity nitric acid forms fumes. Above 95% nitric acid the solution is called white fuming nitric acid. There are several ways to remove the yellow color to make clear white fuming nitric acid, such as bubbling air through the mixture. [48] This was not necessary for this research as it has a downside of producing more toxic fumes.



2.4 Characterization Techniques

2.4.1 UV-Vis spectroscopy

As an indicator for stability UV-vis spectroscopy was used in this thesis. With this technique it was possible to analyze the absorbance at a wide range of wavelengths for $\text{Pd}(\text{NO}_3)_2$ and $\text{Ni}(\text{NO}_3)_2$ at different concentrations of nitric acid (or only in water). The technique is easy as ultraviolet and visible light are emitted through the cuvette and is compared with the amount of light that comes from the source. The difference in light intensity is then the amount of light absorbed by the sample and is given for each wavelength between 200 and 800 nm approximately.

When analyzing the bimetallic 5 wt%, the same concentration used for precursor solutions in synthesis, metal precursor solution with a 90/10 ratio of Nickel nitrate and Palladium nitrate it was possible to use a cuvette with 1 cm in diameter. When only going for a Palladium nitrate precursor solution at 5

wt%, it is not possible to detect emitted light from the important absorbance areas due to strong absorbance of the light by Palladium ions. Therefore, a smaller cuvet of 0.1 cm can be used to measure the 5 wt% of Palladium.

To compare different concentrations and/or cuvet lengths the Lambert-Beer Law was used, see equation 9. [49]

Equation 9: $Abs = \epsilon * b * c$

Equation 9: Lambert-Beer law, where Abs is the absorbance, ϵ is the molar absorptivity in L/mol/cm, b is the path length in cm and c the concentration in mol/L

Absorbance A is calculated computational by the UV-vis program, see equation 10. The program can measure the absorbance up to 4, which means that up to a difference of 1/10.000th between the emitted and measured absorbance signal can be measured. Analysis of these areas learns that these values are not that accurate, but below an absorbance of 3 should still be fine, which is a 1/1.000th of the emitted signal.

Equation 10: $A = \log \frac{I_0}{I}$

Equation 10: Calculation of the absorbance, where A is the absorbance, I_0 is the amount of light that is emitted by the light source and I is the amount of light that goes through the sample.

2.5.1.1 UV-vis of Palladium nitrate in Nitric Acid

In total, three peaks can be assigned due to Palladium interaction in the UV-vis region. [50] Due to strong interactions and overlapping peaks, it is difficult to obtain a clear view of all three peaks together. In figure 7, one peak is observed and the formation of a small bump towards another peak at higher concentration of nitric acid. For Palladium nitrate in 1.0M HNO₃ the following peaks are expected:

- 230 nm: Absorbance is due to a mixture of Ligand to Metal Charge-Transfer (LMCT) and Metal-Ligand Charge-Transfer (MLCT) transitions.
- 295 nm: Absorbance is due to Ligand to Metal Charge-Transfer (LMCT) transitions.
- ~400 nm: Absorbance arises from 4d⁸ intra-transitions between multiplet energy levels. For Palladium nitrate the molecular orbitals are composed mainly of Pd-4d orbitals. The molecular orbitals are split into five levels, where the lowest two consist of almost the same energy at -6.88/-6.97 eV as well as the two transition states above there, at -5.44/-5.58 eV they have almost the same energy. [51] In ground state, the four levels are filled with electrons and the

highest energy level, at -1.76 eV, is empty. When charged with energy (light) an electron can be transitioned from one of the lowest energy levels to the highest energy levels generating absorbance around 400 nm.

- In the range of 550-600 nm also transitions due to the configurations sketched above can be attributed, but because the transition is spin-flipped not experimentally visible. [50]. Moreover, at 200-320 nm absorption is expected for the same transitions but are not visible because they are considered weak and the charge-transfer transition is reasonably stronger.

Peaks < 320 nm are influenced by HNO₃ concentration and show an increase at increasing HNO₃ concentration. An increase is found at those peaks when concentration of HNO₃ is increased. Therefore, analyzing these lower peaks is difficult and the peak at around 400 nm is used.

The paper of Wanatabe et al [50] suggests that depending on the Pd complexes present (and the concentration of those) the peak at ~400 nm is shifting due to change in concentration of HNO₃ and therefore the pH. The reason for this observation is the permittivity of HNO₃. The shift is small and therefore the complex undergoes minor changes. The maximum of this peak in the study of Wanatabe et al ranged from 385 nm at 1M HNO₃ to around 405 nm at 6M HNO₃. Different studies show similar results but also show differences in the exact maximum of these peaks. This counts also for the absorbance, in some studies the absorbance is at the same level, in other studies the absorbance increases at increasing concentration of nitric acid, see figure 6.

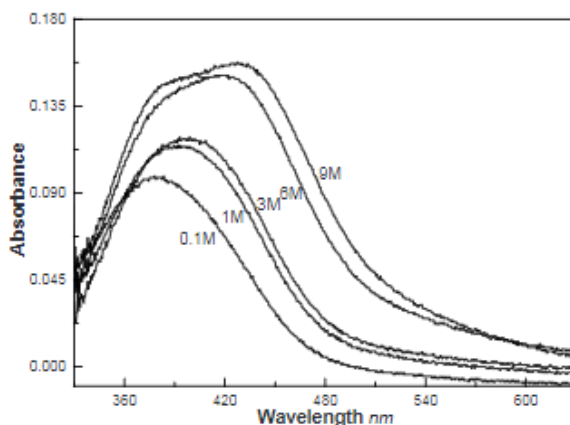


Figure 7. Absorption patterns of 0.5 mM Palladium (II) ions in different concentrations of nitric acid, adapted from [52].

2.5.1.2 UV-vis of Nickel nitrate in water

For analyzing the bimetallic system of Nickel and Palladium in UV-vis the spectra of Ni(NO₃)₂ is necessary. At different concentrations of HNO₃ Ni²⁺ ion shows the same absorption and peak points in UV-vis for the area that is not influenced by HNO₃. Only the peaks < 320 nm, as was for Palladium

nitrate, are influenced by HNO_3 . Therefore, $\text{Ni}(\text{NO}_3)_2$ was dissolved in water and analyzed with UV-vis, see figure 7. The data obtained was compared with other results from different studies and peaks were denoted with the Tanabe-Sugano diagram for octahedral d^8 electron configurations, see figure 8. [53] [54] The peak at 300 nm is due to absorbance of HNO_3 . This peak is more outstanding as Nickel is not absorbing in that region.

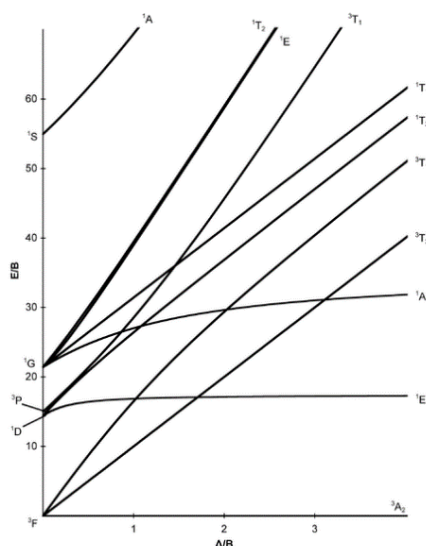


Figure 8. Tanabe-Sugano diagram for octahedral d^8 metals. The different lines show the energy of the transition at different configurations of Δ , which is the crystal field parameter. For $\text{Ni}(\text{NO}_3)_2 \cdot 6\text{H}_2\text{O}$ the energy is around 950 cm^{-1} and for $\text{Ni}(\text{NH}_3)_6(\text{NO}_3)_2$ this is higher at around 1100 cm^{-1} . The lowest energy level is found at 3A_2 and is the ground state of the d^8 configuration.

The double maximum at 655 and 724 nm is due to potential energy surfaces of the coupled E_g states that cross in a region close to the starting position of the wavefunction. [53] The result is an important transfer of amplitudes at short times, which leads to two maxima in the absorption spectrum.

2.5.2 X-ray diffraction

For identifying the crystalline phase of supports and calculating their metal particles sizes X-ray diffraction (XRD) was performed. XRD is a method to analyze powder in finding the phase of crystalline materials and information on unit cell dimensions. The measured XRD signal is compared to a known pattern for this crystal. Moreover, the probability in how likely this species corresponds to known values of the measured XRD pattern to certain crystalline patterns can be given. Together, the obtained pattern is compared to known patterns computational as visibly. X-rays are generally generated by a

cathode ray tube and a diffraction pattern is measured when Bragg's Law has met the requirements, see equation 11.

$$\text{Equation 11: } 2d (\sin\theta) = \lambda_0$$

Equation 11: Bragg's Law, where d is lattice spacing in a crystal in nm, θ is X-ray incidence angle also called the Bragg angle and λ_0 is the wavelength of the x-ray.

For analyzing the particle size, the Scherrer equation can be used, see equation 12.

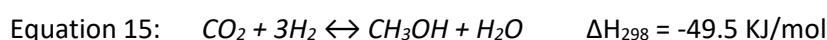
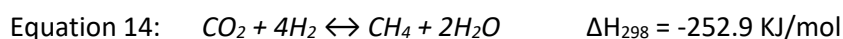
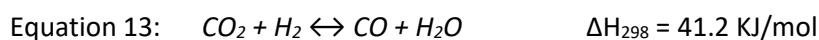
$$\text{Equation 12: } \tau = \frac{K \cdot \lambda}{\beta \cdot \cos\theta}$$

Equation 12: Scherrer equation, where τ is the mean size of the crystalline domains in nm, K is the shape factor and a common value of 0.89 is used for cubic systems, λ is the wavelength of the x-rays and for Co-K α the wavelength is 1.79Å, β is line broadening at half the maximum intensity (FWHM) and θ is the Bragg angle.

2.5.3 Catalytic testing on operando system

For analyzing the catalytic behavior of a catalyst, a continuous flow system together with infrared spectroscopy (IR) and gas chromatography (GC) are used and are discussed in this section. The term operando suggests that the catalytic activity is measured at the same moment the catalyst is in use, which has as a benefit that catalytic data can be analyzed more specifically than in batch process.

In this study, the conversion of CO₂ into methane is used as a basic reaction to test the hydrogenation activity. This will help develop working catalysts. There are different reactions that compete during catalytic testing, see equations 13, 14 and 15. [55]



Diffuse reflectance infrared Fourier transform spectroscopy (DRIFTS) was used as an alternative to the continuous flow reactor. Downside of this method was that it is difficult to measure the activity for (exactly) the same amount of catalyst and that the time to test the catalyst is limited as the detector needs to be cooled with liquid nitrogen and does not function when the nitrogen is gone.

3. Experimental

3.1 Chemicals

Nitric acid	(HNO ₃ 68%)	VWR Chemicals
Palladium nitrate	(Pd(NO ₃) ₂ x·H ₂ O)	Sigma-Aldrich
Potassium nitrate	(KNO ₃)	Acros Organics
Sulfuric acid	(H ₂ SO ₄ 98%)	Supelco (Merck)

3.2 Synthesizing (fuming) Nitric acid

Highly concentrated (fuming) nitric acid was made in a simple distillation setup, containing a condensation column and a flask to catch up the distillate, see figure 10. The flask, containing the fuming nitric acid, was cooled with ice and the condensation column contained running water. Potassium nitrate (Sigma-Aldrich) was pre-dried, using vacuum, to remove any water present, and added to the reaction flask. Sulfuric acid (98%) was added directly inside the distillation to prevent the instant formation of NO_x gasses outside the distillation column. Five washing bottles were used to prevent NO_x and other acidic gases from escaping into the air. Four washing bottles were connected in a way that liquid can't escape and contained a NaOH solution with a bromothymol blue indicator and one with water. A fifth washing bottle was used and contained only water. Over the reach of the experiment the first washing bottle containing NaOH solution was turning clear, indicating formation of acid gases.

The formation of unwanted NO_x gasses was limited by covering the glass components, containing nitric acid, as often as possible with aluminium foil and turning the lab-light off.

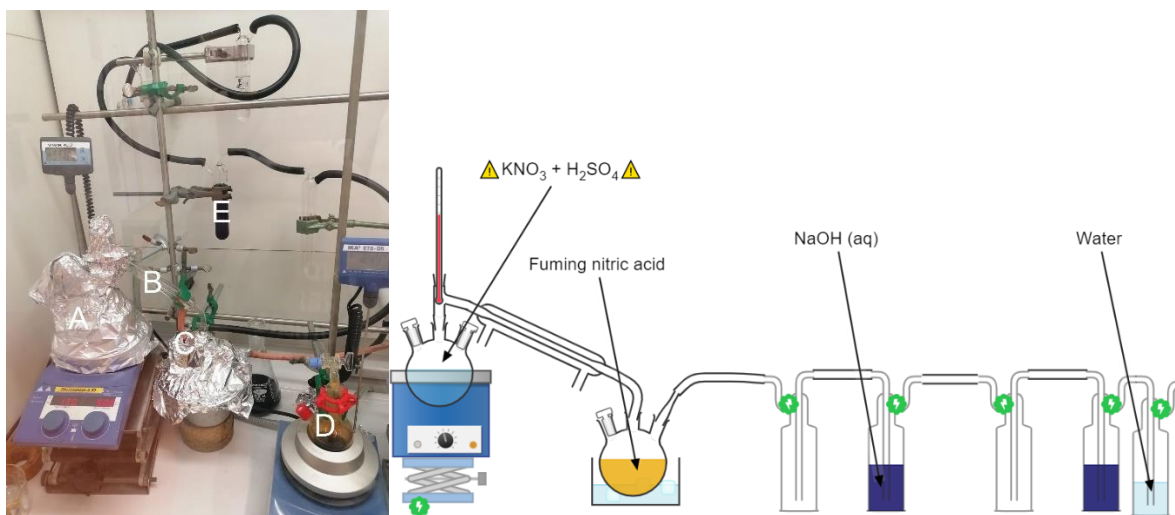
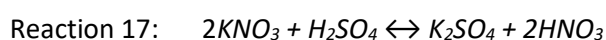
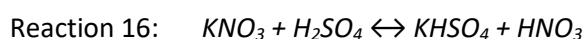


Figure 10. Set-up for making fuming nitric acid, **a** round bottomed flask, connected to **b** condensed cooler filled with running water, connected to **c** a round bottomed flask cooled in ice, **d** contains $\text{Pd}(\text{NO}_3)_2$ dissolved in the fuming nitric acid from **c** and **e** shows the washing bottles containing NaOH solution.

The synthesis was adapted and optimized during several tests from [56]. A 500 ml round bottomed flask was filled with 192 g of KNO_3 and before the start of the synthesis 225 g of H_2SO_4 . During reaction nitric acid is formed and KHSO_4 , which is a white solid at room temperature and a liquid at operation conditions, see reaction 16. Twice the amount of sulfuric acid as Potassium nitrate was added to obtain an oversaturation for sulfuric acid. This oversaturation of sulfuric acid prevents the full conversion towards K_2SO_4 , see reaction 17. The formation of Potassium sulfate is prevented because the boiling point is around the boiling point of nitric acid, resulting in evaporation of the compound and polluting the nitric acid. [56]



The mixture had an exothermic reaction directly after adding sulfuric acid. Due to the heat formed by this reaction, nitric acid fumes are instantly released from the mixture. A heater was used to retain the temperature stable at 83°C head temperature (indicated by the thermometer). Over time, the amount of nitric acid formed in the distillation column and the head temperature was decreasing. Therefore, the temperature of the mixture was increased to progress the distillation. Average formation of nitric acid was around 1 drop every 5-10 seconds. When the evaporation and condensation of nitric acid was slow the column turned orange, but when there was a controlled flow of condensed nitric acid the column was clear, resulting in yellow/orange nitric acid at the end of the column. The full process took 3 days of constant production of drops of fuming nitric acid during daytime. Overnight the reaction

was turned off and the nitric acid was kept in a fridge at -20°C. This was done to hinder light absorbance and heat and therefore formation of acidic gases. The next day new ice was added and the reaction started up again.

3.3 Recrystallization of Palladium nitrate

Recrystallization procedure based on [57].

3.3.1 Using fuming nitric acid

A 100 ml round bottomed flask was filled with 0.6 g Palladium nitrate (Sigma-Aldrich, 205761-10G, Lot# MKCM4344) and cooled with ice. Every two hours the produced fuming nitric acid was added with a glass pipette to the Palladium nitrate. This was slowly stirred to increase dissolving of Palladium nitrate. Overnight the flask was stored at -20°C. After three days of adding nitric acid and stirring, the flask was put under vacuum to remove the nitric acid and water. Under continuous stirring the flask was dried at room temperature. During vacuum drying, the first part of the nitric acid was removed due to boiling of the solution. Later the solution stopped boiling and the rest was dried below the boiling point of the solution. After all the solution evaporated, the palladium nitrate was kept in a vacuum for some hours (2-3) to ensure all the water was removed. The palladium nitrate was scraped from the bottom and ground to a fine yellowish powder.

3.3.2 Vacuum drying

A setup was made to prevent any toxic and acidic gases from entering the pump and atmosphere, see figure 11. Therefore, two cold traps and a solid NaOH trap, to neutralize the acidic gases, are used. The cold traps are cooled down with liquid nitrogen. The evaporated nitric acid is solidified inside the first cold trap and any fumes that could pass through can be caught inside the second cold trap. The first cold trap was emptied from time to time to prevent clogging. A Schlenk line was used and the average vacuum that was reached was 0.03 bar.

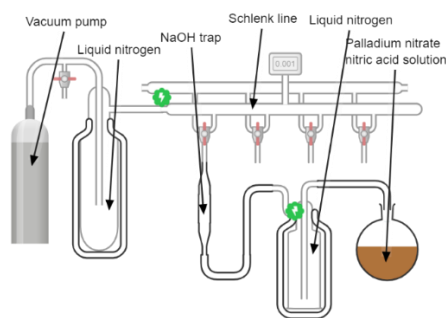


Figure 11. Set-up for evaporating nitric acid from Palladium nitrate solution. A Schlenk line, with two cold traps and an acid trap was used.

3.3.3 Using concentrated nitric acid

For the palladium nitrate that was recrystallized with concentrated nitric acid, 150 ml 68% nitric acid (Sigma-Aldrich) was used to dissolve 0.6 g Palladium nitrate (Sigma-Aldrich, 205761-10G, Lot# MKCM4344). The flask was stirred for two days and then dried in a vacuum. The same set-up was used as for the fuming nitric acid, see figure 11. The temperature was slowly increased starting at room temperature. In the end the temperature was set at 60°C to induce boiling. The first day, the temperature was only increased to 40°C and the second day to 60°C, because hardly any nitric acid was evaporated.

3.4 Synthesizing Palladium on SiO₂ catalysts

A short description of the single steps for synthesis of Pd/SiO₂ catalysts ready for catalytic testing are shown in figure 12.

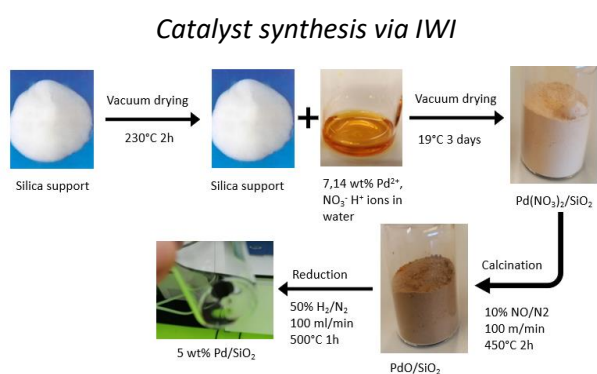


Figure 12. Method for catalysts synthesis by incipient wetness impregnation, calcination and reduction, discussed in this section.

3.4.1 Impregnation of precursor solution on support

Different catalysts containing Palladium and/or Nickel were synthesized via incipient wetness impregnation on the two different supports: CARiACT and BASF. The solutions needed for impregnation were made in vials of around 10 ml in which a particular amount of $\text{Pd}(\text{NO}_3)_2 \cdot x\text{H}_2\text{O}$ and/or $\text{Ni}(\text{NO}_3)_2 \cdot 2\text{H}_2\text{O}$ was added. Around 1-2 g of support was used each time a catalyst was synthesized. The silica support was pre-dried in a round bottomed flask with a syringe rubber at 230°C for two hours at vacuum with constant low speed stirring. Then cooled down to room temperature before impregnation. The precursor solution was made with 7.14 wt% Palladium to compensate for the 0.7 ml/g possible uptake of the support for BASF to have a total of 5 wt% metal needed for CARiACT support. For impregnation, a syringe with a long needle was used to reach the support. The syringe was filled with the precursor solution and the bubbles were removed from the syringe. Before impregnation, the vacuum valve was closed and the needle was bent to 90° to prevent that all the precursor solution was impregnated directly. During impregnation, the precursor solution is slowly dropped into the flask with stirring of the support in a way that the solution can reach every particle. The support containing the precursor solution was dried overnight for at least 3 nights.

3.4.2 Calcination and reduction of impregnated support

Around 0.5 g of dried catalyst was calcined in a fluid bed reactor at 450°C for 2 hours with 10% NO/N_2 of a total of 100 ml/min. The thermocouple was put aside the reactor, without touching the heating lines. From this 0.5 g was around 0.1 g calcined catalyst reduced at 500°C for 1 hour with 50% H_2/N_2 at 100ml/min. Because of the limited amount of catalyst that was reduced it was not necessary to use a fluid bed reduction. The thermocouple was put aside the reactor, without touching the heating lines.

3.5 Characterization techniques

3.5.1 UV-vis

Different concentrations of Palladium and nitric acid were put in 0.1 cm glass cuvette. A program was used that measured the samples every 3 minutes and slow measurement time was used. First, a background was made from water and the cuvette and then the source was blocked to prevent any

light reaching the detector. After this, the cuvette should be filled with the sample. The time between synthesizing the sample and testing was limited as short as possible. When a sample was stable for at least 30 min, or the certain peak outran the maximum measurable value, (absorbance of 4) the measurement was stopped.

3.5.2 XRD

For this thesis, XRD patterns of calcined and reduced catalyst and Palladium nitrate salts were made in a Bruker AXS® D2 Phaser (2nd generation) diffractometer using Co-K α radiations operating at 30 kV with a current of 10 mA at room temperature. A fixed slit was used. Samples of calcined and reduced catalyst were scanned over a 2θ angle ranging from 37° to 57° with a step size of 0.05° and 6 s/step. In this range two significant peaks for PdO as well as for lone Pd can be observed, same story in analyzing NiO and Ni. The Palladium nitrate salt is analyzed over a broader range, ranging from 10° to 90° with a step size of 0.05° at 1.7 s/step. For calcined and reduced catalysts as well as Palladium nitrate was analyzed by a wide aperture where the catalyst was put on and a glass screen was used to homogenize and randomize the sample. For Palladium nitrate the aperture was first filled with a non-measurable silica support where the Palladium nitrate was put on, afterwards homogenized and randomized as with the catalysator.

Using the Sherrer equation, a clear indication for the particle size in the catalyst can be obtained, though the method does not find the size distribution. For measuring the particle size with the Scherrer equation two different methods were used. For the first method a program on the XRD-computer was used to define β and directly calculated the mean size from this value with the Sherrer equation and the same factors. The second method was measuring β with a program called Origin. The intensities at different angles were put in manually and the program could calculate β from the function it calculates, see figure 9. The Scherrer equation was then used on the values that were created by Origin. The average error value given for his method is around 0.06 nm. The computer program for the first method does not give an error value. Therefore, the error is around the same because in a similar way the particle size is calculated by the two methods. The reason two methods were used was to generate more trustful results and not every method makes it possible to calculate every peak. That is because some peaks are not recognized when the peak is broad and low.

For analyzing the recrystallized Palladium nitrate, the measured pattern was compared with patterns for Palladium oxide and Palladium nitrate available on the server, see figure A1 and A2.

3.5.3 Catalytic testing

The calcined catalyst is put into the DRIFTS reactor and the gas lines are connected to the inlet and the outlet. The inlet is connected with a gas feet, which controls which gases and the amount of gases are entering the reactor. For analyzing the activity of the catalyst, the outlet is connected to a gas chromatographic (GC) analyzer. First, the calcined catalyst is reduced at 550°C for 1h with 20 ml/min H₂/N₂ (50% v/v). After that, the temperature is decreased to 250°C which is the first measuring temperature point. As a second step is CO₂ added to the flow together with H₂/N₂. As mild conditions are used, the pressure stays constant, at around 1 atm. At different temperatures, ranging from 200°C to 450°C, the activity is measured. During 45 min the activity for CO₂ hydrogenation is measured with a gas flow containing 20/16/4 ml/min for He/H₂/CO₂. The same was done at 250°C, 300°C, 350°C and 400°C. When using a DRIFTS cell, the program was shortened to make it possible to be cooled with liquid nitrogen, without all the liquid nitrogen evaporating before the end of the program. The program was the same except 250°C and 300°C were skipped, to make sure the detector was still cooled. During catalytic testing IR, TCD and FID were used. Pressure was constant at around the standard pressure of 1 atm. GHSV is 10⁵ h⁻¹.

For analyzing the amount of methane produced, the absorbance at the wavelength of methane is measured in IR and compared with a calibration line. Together with gas-law is the total amount per minute calculated. A percentage is given on the amount of methane produced of a total of the maximum amount of methane possible from reaction with CO₂ and H₂.

Equations 18, 19, 20 and 21 were used to calculate the conversion as well as the selectivity of the catalytic process.

$$\text{Equation 18: } \textit{Feed Conversion} = \frac{\textit{Feed before reaction} - \textit{Feed in products}}{\textit{Feed before reaction}} \times 100\%$$

$$\text{Equation 19: } \textit{Product yield} = \frac{\textit{Carbon mass of product}}{\textit{Carbon mass of feed}} \times 100\%$$

$$\text{Equation 20: } \textit{Selectivity} = \frac{\textit{Yield}}{\textit{Conversion}}$$

$$\text{Equation 21: } \textit{TOF} = \frac{\textit{Total amount of product formed per second}}{\textit{Total mass of metal in catalyst}}$$

4. Results and discussion

During diverse experiments on Palladium nitrate, ones consisting of a stability diagram for Palladium ions, a new source of Palladium nitrate was used. The Palladium nitrate source, consisting of deviating characteristics, formed particles sooner than was expected from previous results by the old source. Therefore, it was not possible to make a useful stability diagram of just Palladium nitrate in the different forms, see figure 6, and nitric acid concentrations available. Palladium nitrate had to be adapted to make experiments and results widely applicable for future synthesis of Palladium catalysts. Otherwise, the characterization and performance is too dependent on the quality of the Palladium catalysts. Data from Sigma-Aldrich showed a large variety of different batches for Palladium nitrate ranging between 39% and 41% of Palladium metal, see figure A3. The first source had a theoretical value for Palladium concentration of 39.1% and the second source consisted of 41.0% Palladium metal. which was not checked with ICP-OES. The observed difference between different qualities of Palladium nitrate was visible in the color of the powder; the more concentrated Palladium nitrate source contained a darker brown powder than the 39.1% Palladium, see figure 13. Moreover, in the 41% Palladium source bright crystals were visible, which could be an indication to solid Palladium metal and/or Palladium oxide present in the powder. As described in the theory section, solid Palladium and Palladium oxide tend to sinter into larger particles and prevent Palladium from entering the pores, as the particles are already too large. Therefore, the first part of the results section is on recrystallization of Palladium nitrate by fuming nitric acid. The second part is about characteristics and comparison of the newly formed Palladium nitrate to the old source.



Figure 13. Two types of $\text{Pd}(\text{NO}_3)_2 \cdot x\text{H}_2\text{O}$ on top of each other. The lighter brown is the first batch containing 39.1% Pd and the darker brown powder contains the batch with 41% Pd.

The UV-vis experiments described later, were performed on the first batch of Palladium nitrate (39.10% Pd) and were reproduced on the source containing 41% Palladium metal one in making a stability diagram. The catalyst used in operando IR containing the non-recrystallized Palladium nitrate also contained the 39% Palladium nitrate.

4.1 Synthesizing fuming nitric acid

As there was not a clear way of making nitric acid from literature reviews and patents, nitric acid was first synthesized in small quantities to test the purity and performance. These results were used to optimize the reaction conditions. The temperature needed to reach the sufficient head temperature was altered to the values discussed in the experimental section. During this testing phase, a less concentrated Sulfuric acid (90%) solution was used and Potassium nitrate was not pre-dried. The first tests resulted in nitric acid with a density of around 1.41 g/ml, calculated from measuring the volume and weight. The density of nitric acid is compared with known values of nitric acid at different temperatures and corresponds to around 70% of nitric acid purity. [58]

The optimized conditions, consisting of 98% Sulfuric acid and the dried Potassium nitrate, resulted in more intensely fuming nitric acid and the density increased to around 1.51 g/ml. This density corresponds to 98-99% purity, which is significantly purer than during the testing phase. The pure fuming nitric acid colored yellow/orange and was a bit darker than during the testing phase.

4.2 Recrystallization of Palladium nitrate hydrate

The synthesized fuming nitric acid, containing a concentration of around 98-99% was added to the Palladium nitrate. It was difficult to exactly measure the amount of nitric acid produced, because it will lose its purity every time the solution is put in light. The solution was dark brown/black and was stirred continuously during the day. After all the nitric acid was added and all was stirred thoroughly the solution was dried at the Schlenk line set-up.

The dried and recrystallized Palladium nitrate was removed from the round bottomed flask and showed a light brown colored solid without bright chunks, see figure 14. The formed Palladium nitrate has an even lighter brown than the Palladium nitrate at 39%. The solid Palladium nitrate powder was analyzed by X-ray diffraction and compared with known Palladium nitrate hydrate and Palladium oxide diffraction data, see table A1 and figure A1 and A2. The obtained diffraction patterns were put in a figure in order of likeness and conformity to Palladium nitrate or Palladium oxide, see figure 15.



Figure 14. Recrystallized $\text{Pd}(\text{NO}_3)_2$ with fuming nitric acid agent, dried in vacuum. No bright chunks of Palladium or Palladium nitrate are visible any more.

XRD patterns of Palladium nitrate samples and theoretical patterns.

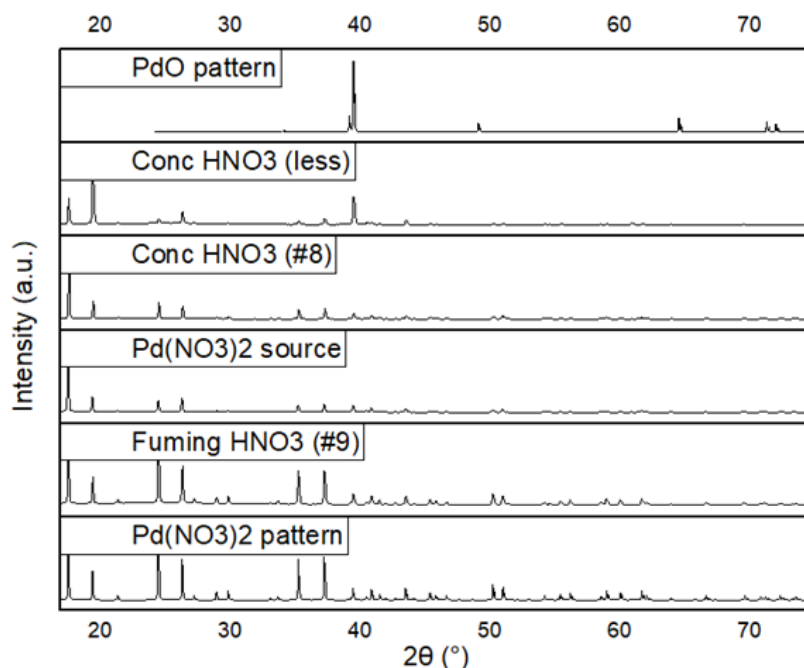


Figure 15. XRD results from analysis of the recrystallized $\text{Pd}(\text{NO}_3)_2$ together with the corresponding PdO and $\text{Pd}(\text{NO}_3)_2$ theoretical patterns above and below, from figure A1 and A2. The diffraction patterns are ordered on likeness towards PdO or $\text{Pd}(\text{NO}_3)_2$.

Different Palladium nitrate samples are compared with each other. Using a small amount of nitric acid on an old Palladium nitrate solution, some of which showed many particle formation, led to high conformity towards Palladium oxide, see “Conc HNO_3 (less)” signal in figure 14. This is mostly visible at the peak around 39° . The species shows peaks lower than 20° , but the intensities are reversed as visible in the Palladium nitrate pattern. When using more concentrated nitric acid as a recrystallizing agent, more conformation towards Palladium nitrate is observed. The two peaks below 20° are more closely to the ratio of the Palladium nitrate pattern. Moreover, the peak at 39° is significantly lower, making sure a lower percentage of Palladium oxide is in the species. Also, this peak is almost comparable to the peak of Palladium nitrate without any recrystallization, showing that using nitric acid as a recrystallization agent and performing recrystallization is not a sufficient method to improve the purity towards Palladium nitrate. If this has led to an even worse ratio between Palladium nitrate and Palladium oxide Rietveld analysis should clarify.

A total low conformity towards both species, observed for both the Palladium nitrate source and recrystallized with concentrated nitric acid, could be caused by some reasons. First, the signal could be low at the cost of the total conformity towards one of the patterns, as the corresponding patterns do not have the same intensity ratio of peaks and/or together with the low intensity of the single peaks

makes the noise level more significant. This can be caused by diluting the sample too many times with a non-observable support or randomizing the sample poorly, which results in observing only some sides of the sample. Another reason could be that the sample was not dry enough and low amounts of crystals were observed because of that. Previous found results from XRD, with low intensity peaks, were remeasured and the amount of used sample was increased which gave, in the most cases, an improved result in most of the cases.

Using fuming nitric acid, on the other hand, shows a close conformity towards the Palladium nitrate pattern. The ratio between the peaks lower than 20° are not optimal yet, but the method is promising. Also here, Rietveld analysis will clarify in what way the fuming nitric acid contributed to the formation of pure Palladium nitrate. Indeed, when using fuming nitric acid, which has low water availability, in reaction 5 balance is more towards the Palladium nitrate and water. The amount of formed water can be calculated from the concentration of Palladium nitrate, which can be found by Rietveld analysis and the amount of Palladium nitrate used.

These results show that indeed using fuming nitric acid gives a higher concentration of Palladium nitrate than using concentrated (68%) nitric acid with more volume. The conformity towards pure Palladium nitrate could probably increase even more when more fuming nitric acid is used, but the difference it has made was already significant. It would be interesting to do the recrystallization once again with fuming nitric acid and measure the confirmation towards Palladium nitrate with Rietveld analysis.

An optimum in percentage of Palladium inside Palladium nitrate hydrate, and therefore an optimum of water molecules per molecule, could lead to an optimum in stability. This effect has been observed, but it is difficult to conclude if this instability arises from the metallic shiny parts found in the second (41%) Palladium nitrate source, which were not observed in the first source. If this was just a failure from Sigma-Aldrich that delivered the Palladium nitrate or other Palladium source also contained shiny parts is unknown. Analyzing the salt with different characterization methods and analysis should give some exclusions on what exactly determines Palladium nitrate to be unstable.

4.2 ICP-OES

Next to XRD (and possible Rietveld analysis), which shows and measures the concentration of Palladium nitrate and Palladium oxide, Inductively Coupled Plasma-Optical Emission Spectroscopy (ICP-OES) can be used to give an indication on the amount of Palladium metal present in the powder.

The results show how well the crystallization is performed (in terms of Palladium percentage) as the availability of contaminants. This ICP-OES is performed outside the Inorganic Chemistry and Catalysis group and was also used for catalysts to measure the concentration of metals inside and what kind of contaminants are present that could hinder the catalytic activity of the sample. The sample is destructed by aqua regia to dissolve all the metals and the signal of the solution is compared with calibration signals of known metals.

From ICP-OES data the concentration of Palladium metal in the recrystallized Palladium nitrate is calculated. Using concentrated nitric acid as a recrystallization agent a total of 35.3% of Palladium metal is measured after recrystallization. Using fuming nitric acid as a recrystallization agent led to 40.7% of Palladium after recrystallization. Considering an complete dry salt the 40.7% Palladium results in the $\text{Pd}(\text{NO}_3)_2 \cdot 1.73\text{H}_2\text{O}$ structure. Compared to 41% and 39.1% Palladium concentration of the original salt, which corresponds to $\text{Pd}(\text{NO}_3)_2 \cdot 1.62\text{H}_2\text{O}$ and $\text{Pd}(\text{NO}_3)_2 \cdot 2.32\text{H}_2\text{O}$ respectively, the fuming recrystallized salt comes close to the original value of 41% and is in between the two concentrations. Using concentrated nitric acid leads to high value for water molecules far from close to the original value and was therefore not given in a structure. Below is discussed why this value of Palladium metal was deviating.

Using nitric acid as a recrystallization agent resulted in low percentage of Palladium and deviates significantly from the starting concentration of Palladium nitrate. As discussed, using concentrated nitric acid instead of fuming nitric acid it is more difficult to make the salt completely dry. This was observed during the vacuum drying stage of the Palladium nitrate recrystallization. The reason for the long nitric acid (and water) evaporation from this Palladium nitrate compound is due to the higher concentration of water and therefore a higher boiling point of the solution. Considering a full dry salt is not accurate for the way this drying stage for this Palladium nitrate was performed, as Palladium nitrate is a known hygroscopic molecule. [59] Moreover, a species that consists of 3.95 H_2O molecules per Palladium molecule is likely as the crystalline molecule exhibits the orthorhombic structure. [60]

Next to the Palladium concentration, ICP-OES data shows the contamination of different metals as well as common elements, which could explain the difference in Palladium concentration as well. Potassium (around 0.017%) and Sulphur (around 0.17%) were found in both the recrystallized species with a slight increase for the fuming nitric acid recrystallization method. Other species were lower in abundance or containing expected values, such as Calcium and Sodium. The total contamination is too small in percentage to explain the difference found in Palladium contribution. Therefore, it is expected that the recrystallized salt, using concentrated nitric acid as recrystallization agent, is not fully dry. From ICP-OES It is not possible to conclude if the high-water level has led to a different salt crystal than using the fuming acid agent. The high availability of Palladium oxide indicates that this could be the case.

4.3 UV-vis

The next part in this thesis is finding out how Palladium nitrate performs in precursor solution conditions. At which concentration of nitric acid optimal stability is found and which recrystallization agent leads to prevention of particle formation. First the absorbance of Palladium nitrate in different concentrations of nitric acid was measured and compared with theoretical (literature) values. The Palladium source used for setting the base was 39.1% Palladium source and a variety of concentrations of nitric acid were used, varying from 1M to 4M, see figure 16. Lower concentrations were not used as they are not in agreement to this figure, that is due to direct formation of particles which increases absorbance. Other concentrations have shown to be stable enough to use as a benchmark for this graph.

UV-vis spectra of 0.5M Palladium nitrate in various nitric acid concentrations.

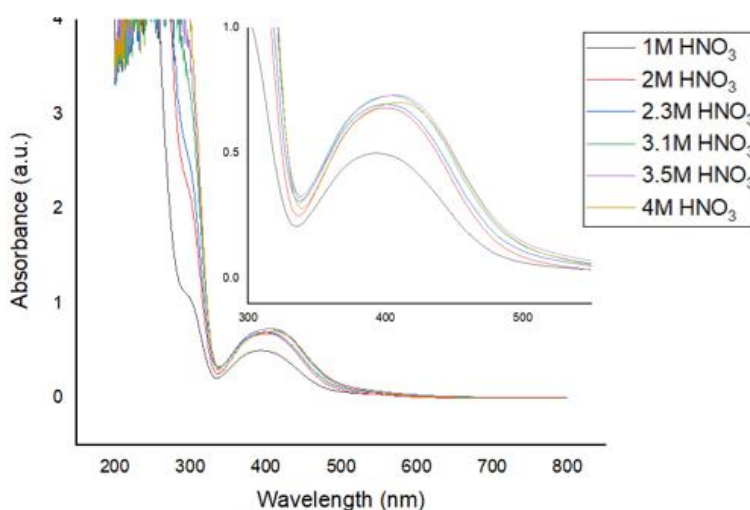


Figure 16. UV-vis spectrum of 0.5M Pd(NO₃)₂ (39.1% Palladium) at different concentrations of HNO₃. Peak at ~400 nm is enlarged. At different concentrations the height of the peak at 400 nm gets more absorbed and shifts to higher wavelength.

The results in figure 16 show that at 1.0M HNO₃ the maximum is reached at 393 nm and this maximum is increasing to 400 nm at 2.0M, 405 nm at 3.1M and 309nm at 4.0M HNO₃. The maximum of these peaks shows another trend. At 1M of nitric acid significantly lower absorbance than all the more concentrated solutions is found. From 2M of nitric acid the absorbance increases slowly to higher absorbance, but 4M of nitric acid shows a lower maximum than in 3.5M of nitric acid. Therefore, it does not completely follow the trend Wanatabe et al suggest. [50] This was expected, because of all

the different trends in other studies. [52] Some reasons that could clarify the difference between the measured and theoretical data are summed below:

1. The concentration of Pd is different. In the paper of Wanatabe et al a concentration of $7 \cdot 10^{-3}$ M is used and $0.5 \cdot 10^{-3}$ M used by Liu et al, which is lower than the 0.5M that is used in this thesis. Therefore, a change in configuration can have a larger influence.
2. It is not clear what kind of Palladium nitrate source they used and how this relates to the source used in this thesis. Therefore, their stability could be different as well as the configuration.
3. From the data in Wanatabe et al a constant height for the peak at 400 nm is found, which is not the case in this thesis data.
4. Literature is not descriptive about materials and probably does not use the same UV-vis spectrometer as well as cuvette, which also leads to differences. Moreover, it is not exactly clear how Wanatabe et al or Liu et al (and other studies), performed their background for UV-vis.

This same behavior experiment was done on Nickel nitrate. There was no influence from nitric acid on the absorbance peaks of Nickel measured, which was expected from theory in the theory section. Therefore, only the influence of Nickel nitrate in water is shown, see figure 17. The only peaks that are affected by nitric acid are below 250 nm.

UV-vis spectrum of Nickel nitrate hexahydrate

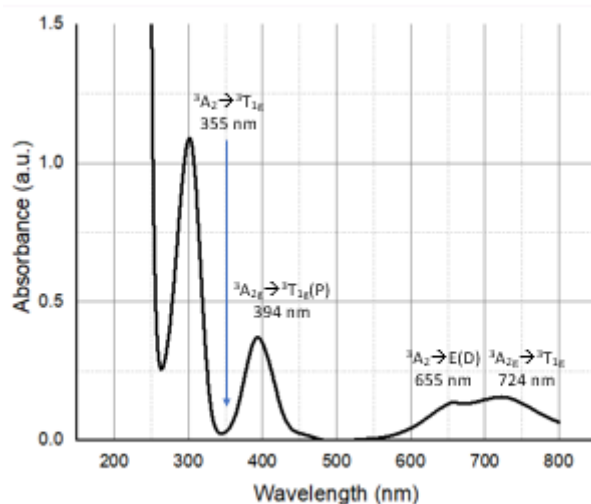


Figure 17. UV-vis spectrum of 5 wt% Ni^{2+} , from $\text{Ni}(\text{NO}_3)_2 \cdot 6\text{H}_2\text{O}$, in water. Above the peaks are the wavelength and the specific transition of the Nickel ion given. Note that the peak at 300 nm is not from the Nickel ion and therefore not indicated.

The absorbance of Nickel nitrate is useful for making stability diagrams for bimetallic Nickel Palladium precursor solutions. Using the Lambert-Beer equation, see equation 9, the total absorbance of used Nickel can be calculated. As the absorbance of Nickel doesn't rely on the concentration of nitric acid, the total contribution of Nickel on Palladium can be calculated.

4.3.1 Stability (old) 39% Palladium nitrate

With UV-vis it was possible to directly analyze the stability of Palladium nitrate dissolved in different concentrations of nitric acid. When 0.1M of Palladium nitrate in 0.1M of nitric acid was analyzed, it imaged the instability of Palladium, see figure 18. An increase in absorbance was measured due to the formation and growth of particles. Therefore, the graph shows the instability of Palladium nitrate in 0.1M nitric acid.

Palladium nitrate in 0.1M of nitric acid over time

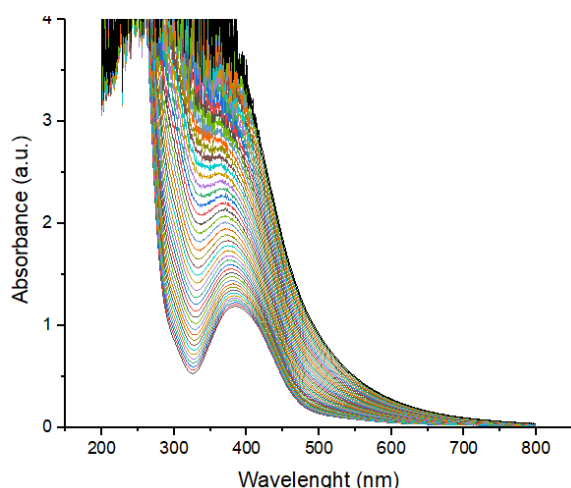


Figure 18: UV-vis spectrum of 0.1M Pd(NO₃)₂ in 0.1M of nitric acid over time. The lowest spectrum is taken at the beginning of the measurement and the highest (black line) at the end of the measurement. The maximum wavelength of the peak is changing from 385 to 365 nm, after the peak at 365 nm no peaks can be distinguished.

The results at 0.1M nitric acid are compared with Palladium nitrate in 1M nitric acid, see figure 19. In the graph the absorbance at 386 nm for the two functions of Palladium nitrate are shown. The absorbance at 1M HNO₃ stays the same and therefore shows a more stable compound. The average slope found at 0.1M of nitric acid is 0.009 abs/min. A straight line at 1M of nitric acid does not mean that no Palladium particles are formed, see figure 20. At 1M HNO₃ large particles on the bottom are observed that are not influencing the UV-vis absorbance. At 0.1M smaller particles are formed that are in suspension in solution and influence the UV-vis signal significantly. Therefore, 1M of nitric acid Palladium nitrate is more stable but not stable enough to completely prevent formation of large Palladium particles. At 0.1M of nitric acid smaller particles are formed.

Absorbance at 386 nm for 0.1M Palladium nitrate in different concentrations of nitric acid precursor conditions.

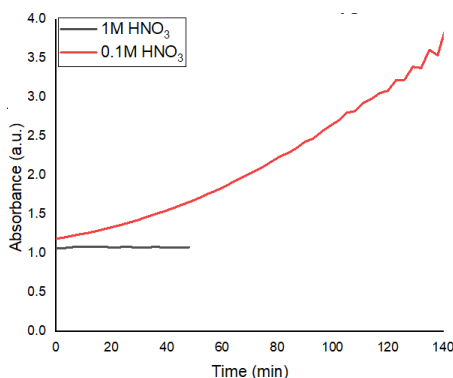


Figure 19: Absorbance at 386 nm for 0.1M Pd(NO₃)₂ (39%) at 0.1M and 1.0M HNO₃. Average slope till 42 min is 0.009 abs/min and 0 abs/min respectively for 0.1M and 1.0M HNO₃.

Different Palladium nitrate solutions containing different concentrations of nitric acid.



Figure 20: From left to right: 0.1M Pd(NO₃)₂ in 1M HNO₃, 0.1M Pd(NO₃)₂ in 0.1M HNO₃ and a 0.1 cm diameter sized UV-vis cuvette filled with 0.1M Pd(NO₃)₂ in 0.1M HNO₃ after UV-vis measurements.

These observations can be explained by the availability of Palladium and/or Palladium oxide particles in the precursor conditions. These particles are not dissolved in solution, instead at 1.0M of nitric acid they grow to significant sizes. At lower concentrations of nitric acid, the formation of similar particles is observed instead of growing, resulting in more but smaller particles in suspension.

4.3.2 Stability (new) 41% Palladium nitrate

For the (new) Palladium nitrate source containing 41% Palladium the same kind of stability experiment was performed as for the 39% Palladium. Directly from the start it was observed that the precursor solution behaved differently from what was observed at the 39%. This was not only the case for a

single concentration, as all concentrations showed a significant formation of particles incomparable to the particles observed at 1.0M of nitric acid at 39%. The same effect was observed at lower concentration where particles are smaller and more existing and at higher concentrations the particles are larger and lower in abundance. This directly led to the conclusion that this 41% Palladium source contained more Palladium and/or Palladium oxide particles that resulted in faster and more formation of particles.

With this conclusion the method for making pure Palladium nitrate needs to be adapted to make it possible to use Palladium nitrate, independently of which concentration of Palladium and the amount of Palladium (oxide) particles existing, the same way. Therefore, recrystallization using nitric acid was developed. This made it possible to improve the Palladium nitrate salt in terms of less available Palladium and/or Palladium oxide particles that resulted in particle formation. If this method also resulted in similar results using different qualities of Palladium nitrate was not checked, which makes it difficult to discuss the repetition of the experiment resulting in the same results. A method to do this is using different concentrations of Palladium nitrate with different amount of Palladium (oxide) particles and measuring after every recrystallization step, or the amount of fuming nitric acid solution used, the amount of Palladium particles formed or a Rietveld analysis from XRD results. This way, the amount of recrystallization, or the amount of fuming nitric acid needed, can be determined, resulting in the worst salt completely turned into pure Palladium nitrate.

4.3.3 Stability recrystallized Palladium nitrate

The stability (e.g. formation of Palladium (oxide) particles) of the newly crystallized Palladium nitrate was tested with UV-vis. The measurement was done for both the fuming and concentrated nitric acid recrystallized Palladium nitrate, both at a high concentration of 1M and at a low concentration of 0.1M nitric acid, see figure 21. The absorbance lines for the Palladium nitrate recrystallized salt with fuming nitric acid in 1.0M and 0.1 HNO₃ in UV-vis spectroscopy.

Stability of recrystallized 0.1M Palladium nitrate by fuming nitric acid.

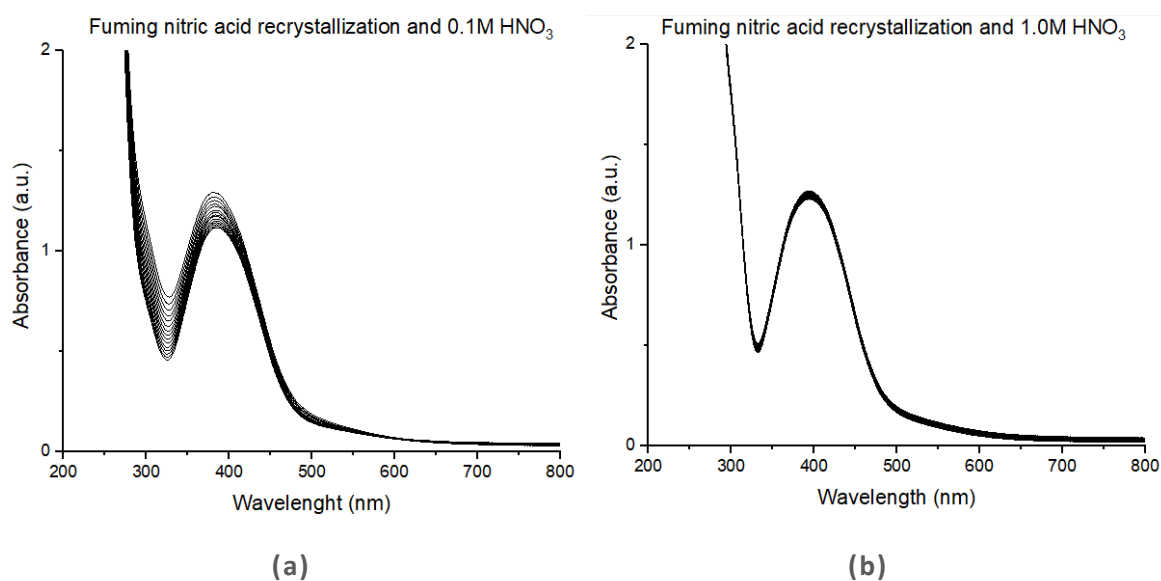


Figure 21. Stability over time of 0.1M Pd recrystallized with fuming nitric acid in **a** 0.1M HNO₃ and in **b** 1.0M nitric acid, recorded by UV-vis spectrometry. At 0.1M of nitric acid the absorbance increases over time and a peak shift to lower wavelength is observed. At 1.0M of nitric the absorbance slowly decreases over time, but the maximum stays on the same wavelength.

The behavior of the two different recrystallized Palladium nitrate complexes was measured over time at different concentrations of nitric acid, see figure 22. The intensity at 386 nm, the wavelength of the peak at the first measurement of 0.1M HNO₃ for the fuming nitric acid method, was taken as standard wavelength for comparison. This wavelength was chosen from figure 21 as the average wavelength of the different maxima shown, it was expected that this wavelength does not lead to changes in the results.

Over 100 min both the different Palladium nitrate at 1.0 M HNO₃ show reasonable stability, as expected. Even after 100 min to 4 hours the absorbance does not change for both the lines (a change around 0.0004 and 0.0001 is small and therefore negligible due to the noise levels). A decrease is observed and measured for the fuming nitric acid recrystallisation at 1M of nitric acid and can be explained by the Palladium nitrate that still was dissolving, as the salt is difficult to dissolve, or that there was some (minimal) Palladium (oxide) present that slowly sedimented to the bottom of the cuvette. The two lines at 1.0M of nitric acid approach each other but never touch. The difference in height between the two could be explained by the slight difference in Palladium concentration (0.015M) as well as the difference in nitric concentration (0.002M) because of the difference in Palladium.

UV-vis absorbance over time of recrystallized Palladium nitrate in different concentrations of nitric acid (and recrystallization agent).

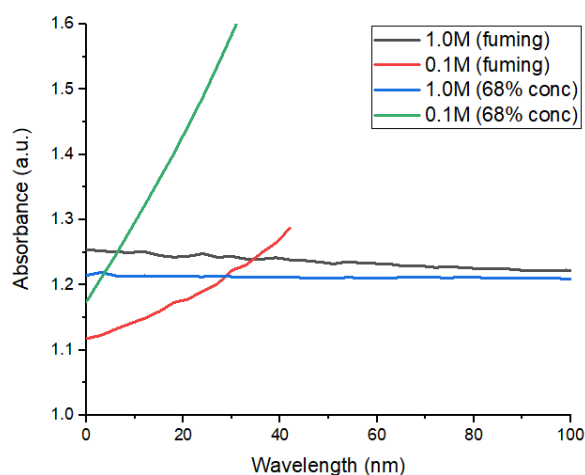


Figure 22. Absorbance at 386 nm over time for the recrystallized Palladium nitrate at different concentrations of HNO_3 . The average slope for these lines are -0.00037 abs/min and -0.00008 abs/min for 1M HNO_3 concentrated and fuming recrystallization respectively. For the 0.1M nitric acid it is 0.004 and 0.015 abs/s for the fuming and concentrated recrystallization, respectively.

The curves of Palladium in 0.1M of nitric acid show a more interesting result than the lines at 1.0M. First, the starting point of both lines are lower than the lines at 1M nitric acid, which is explained by the lower concentration of nitric acid used. As explained before, the nitric acid and Palladium(II) ion absorption line overlaps at certain positions in the spectrum. The curve of the concentrated nitric acid method at 0.1M of nitric acid shows a high increase in absorbance and stays increasing until it reaches the maximum absorbance of the spectrometer. The same effect is seen for the fuming acid curve at 0.1M nitric acid, but the slope is smaller. In the end, this line will also reach the maximum absorbance of the spectrometer. From this it is concluded that the fuming acid recrystallized Palladium nitrate at 0.1M nitric acid shows more stability, in terms of oxidation, than the recrystallized Palladium nitrate with concentrated nitric acid.

The slope for the non-recrystallized Palladium nitrate at 0.1M nitric acid was 0.009 abs/sec, see figure 19. After recrystallization the slope of absorbance at 0.1M of nitric acid is 0.004 abs/sec, see figure 22. This means that after recrystallization with fuming nitric acid the formation and growth of Palladium (oxide) particles is over two times lower than the non-recrystallized Palladium nitrate. For the recrystallization using concentrated nitric acid the slope is 0.015 abs/sec resulting in a formation of almost twice the amount of Palladium oxide. As already discussed in the previous section, the 41%

Palladium nitrate source showed less stability as the 39%, leading to similar or more Palladium (oxide) particle formation as the recrystallized Palladium nitrate with concentrated nitric acid. Though the stability of the recrystallized Palladium nitrate, with concentrated nitric acid, didn't show the same stability as the 39% Palladium source, the stability improved compared with the 41% source. Comparing this with the results found for fuming nitric acid recrystallizing agents, gives this method a significant improvement towards stability of Palladium nitrate. Unfortunately, the result couldn't be compared with recrystallized 39% Palladium nitrate.

4.3.4 Bimetallic precursor stability

This last part of precursor stability is about preference towards bimetallic precursor chemistry. Here the influence of the Nickel nitrate and Palladium nitrate on each other is analyzed. The result of this shows what the influence of the concentration of nitric acid/pH has on the bimetallic precursor solution. Not only the influence of the pH but also the influence of Nickel(II) ions on the formation of Palladium oxide can't be neglected. The area of absorbance shows the instability of the precursor solution and therefore the optimal pH for these conditions. These conditions are 90:10 ratio of Nickel:Palladium and a total of 5 wt% of metal. This is done with the 39% Palladium source and without the recrystallisation process.

This influence is analyzed with the bimetallic as well as both monometallic precursor solutions in the UV-vis spectrometer. For this the spectrum of Nickel nitrate in figure 17 is used. By using the Lambert-Beer law it is easy to calculate the value of Nickel and Palladium at the correct concentration. Then, the total absorption of Nickel and Palladium is removed from the total absorption of the bimetallic precursor solution, see equation 22.

$$\text{Equation 22: } \textit{Influence Nickel and Palladium} = \langle Ni^{2+}Pd^{2+} \rangle - \langle Ni^{2+} \rangle - \langle Pd^{2+} \rangle$$

Equation 22. The influence of Nickel and Palladium ions on each other in a.u.*nm is calculated from the total area of absorbance (the area below the peaks).

The results from equation 9 at different wavelengths can be filled in Origin and the peaks and areas are analyzed. Important is that only the positive values are used for the area from a certain wavelength. All the wavelengths that are influenced by nitric acid are not useful because this influence is twice removed from the bimetallic precursor solution absorbance. Therefore, the wavelength of the peaks that give the influence of Nickel and Palladium are >300 nm, see figure 23. The results obtained are visible in table 3 and shown in figure 24.

Bimetallic influence after removing influence of single Palladium nitrate and Nickel nitrate.

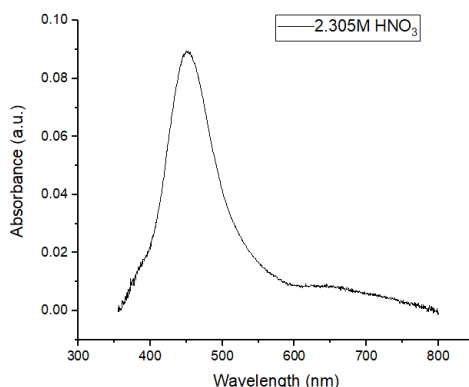


Figure 23. Example of a bimetallic precursor peak that is left when the absorbance of Palladium and Nickel are removed for the same concentration of nitric acid. For this peak the conditions are 2.305M of nitric acid, 90:10 Ni:Pd ratio and 5 wt% of metal. The starting point of the peak is at 350 nm, the wavelength of the absorbance becomes positive.

Results of bimetallic precursor solutions in UV-vis

[HNO ₃] (MOL/L)	AREA (A.U.*NM)	HEIGHT (A.U.)	WAVELENGTH (NM)
0.864	17.139	0.14	433
1.747	10.38	0.093	422
2.305	9.823	0.0896	450
3.496	14.159	0.096	442
4.039	14.688	0.111	456

Table 3. The results from calculating the influence of Nickel and Palladium together at different concentrations of nitric acid, calculated with Origin.

From figure 24 it is observed that the lowest amount of area, and therefore highest stability, is at a concentration of 2M of nitric acid. This gives a clear indication that at a concentration of 2 mol/L of nitric acid, which is a pH of -0.3. Important to note, is that this is the final pH of the precursor solution and not the concentration of the nitric acid that is added to the metal nitrates.

Bimetallic stability at different concentrations of nitric acid.

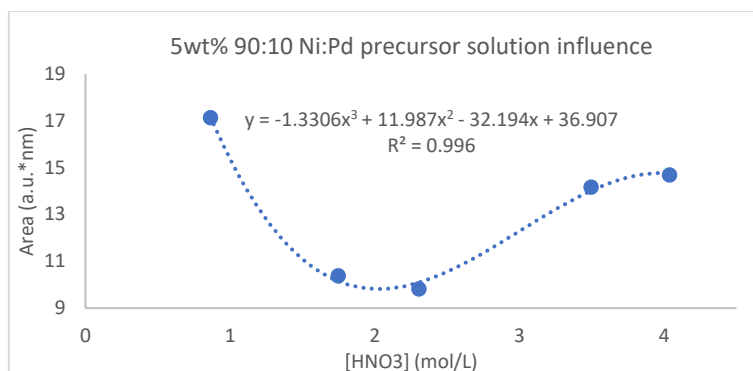


Figure 24. Results from table 3 are shown in blue dots. A trendline is fitted through the points and an order three function is the first order that shows a regression coefficient of 0.996.

A pH of -0.3 does not differ from a pH of 0, at a concentration of 1M of nitric acid, but has a larger consequence in the stability of around 50%. A 0.1M nitric acid solution resulted in a high area of around 35, so it exponentially increases for sure to higher pH. But that does not mean that low concentrations of nitric acid is not doable as is seen in the particle sizes. Moreover, a recrystallized Palladium nitrate salt could lead to a different function but has not been investigated.

4.5 Transmission Electron Microscopy

The next step after generating stable precursor conditions is synthesizing catalysts by method discussed in the experimental section. It is important to prevent any unwanted conditions during the different steps, such as exposure to light and heat. Another important factor is to retain conditions similar and have only one variable that is changed. In this case that is the precursor salt used. Unfortunately, due to several causes it was not possible to analyze both the catalyst containing the original 39% Palladium nitrate precursor solution as well as the fuming nitric acid recrystallized Palladium nitrate. The time between synthesizing the catalyst and performing a Transmission Electron Microscopy (TEM) image of it would be different. As a result, it could be possible that the previous situation, using the non-recrystallized Palladium nitrate precursor solution, would be similar to the new catalysts, synthesized with the fuming nitric acid recrystallized Palladium nitrate precursor solution. Only, when the reduced catalyst was stable, hence no shift of Palladium atoms inside and outside the support as well as sintering, it is possible to compare both the catalysts. As the catalyst was kept at room temperature in an area which is exposed to light it was not trustworthy to draw

conclusions from it. Therefore, no TEM was performed of the reduced catalyst consisting of the fuming nitric acid recrystallized Palladium nitrate.

A non-recrystallized Palladium nitrate catalyst was analyzed with TEM to visualize the fast sintering of Palladium nitrate in nitric acid solution. A 5 wt% Palladium on silica catalyst was made from Palladium nitrate (39%) which was diluted in 1M nitric acid. During preparation, both the nitric acid and salt were cooled at 0°C during mixing and impregnation to prevent rapid destabilization and formation of Palladium (oxide) particles. These lower temperature conditions were sometimes used to see the difference it has on the catalyst, as it was shown on a precursor solution that it took longer for the growth and formation of Palladium (oxide) particles. The impregnated support was calcined and reduced following the conditions discussed in the material section and used regularly. An improvement on the catalyst was not observed, in terms of characterization.

The catalyst analyzed with TEM was considered one of the most stable configurations using the old Palladium source (39%) in 1M nitric acid that showed stability in UV-vis. Therefore, this catalyst can be used as a benchmark for future catalysts made with the new (recrystallized) Palladium nitrate (41%) and in less acidic conditions. If same or improved results compared to this catalyst can be obtained, recrystallizing Palladium would be an efficient step to progress. After processing and analyzing the TEM images with ImageJ a histogram can be made of all the found particles. The catalyst showed a wide spread distribution across the whole support of circular Palladium particles varying from 1 to 17 nm, see figure 25 and 26. In the TEM images are the particles in black and the support in grey.

TEM images of Palladium/SiO₂ before recrystallization using 41% of Palladium nitrate.

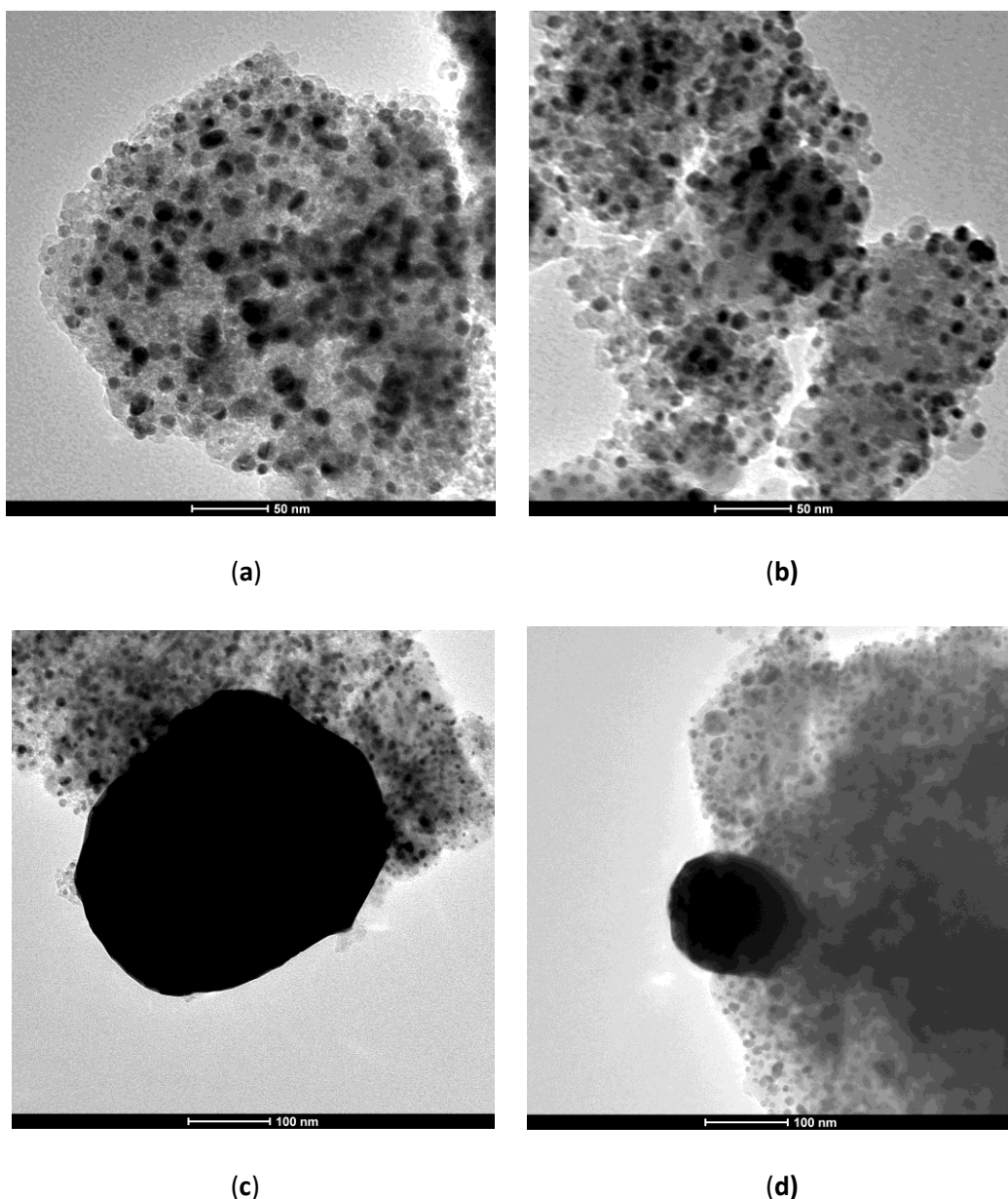


Figure 25: TEM images of 5 wt% Pd/SiO₂ catalyst synthesized from Pd(NO₃)₂ in 1M HNO₃ on BASF SiO₂ support. Normal calcination and reduction conditions were used (described in the method section). Palladium particles are shown as black dots and the Silica oxide supports colors grey. In **a** and **b** wide spread Palladium on silica is visible. In **c** and **d** also wide spread Palladium distribution is observed but also large chunks of solid Palladium on top of the silica is visible.

Overall, a wide spread distribution for Palladium has been found in the TEM and also on the other images that are not shown in this thesis. In the total of 14 images taken the particles are round shaped, but largely differentiating in diameter. Most of the silica support contained particles, but some parts

contained a larger amount of particles. In figure 25a many particles are found inside the support and in figure 25b most of the particles are found outside the catalyst. Unfortunately, also large black dots containing solid Palladium were found on top of the support, see figure 25c and 25d. One of the causes of these large Palladium particles can be devoted to sintering of Palladium metal.

Size distribution from TEM on Pd/SiO₂ catalyst

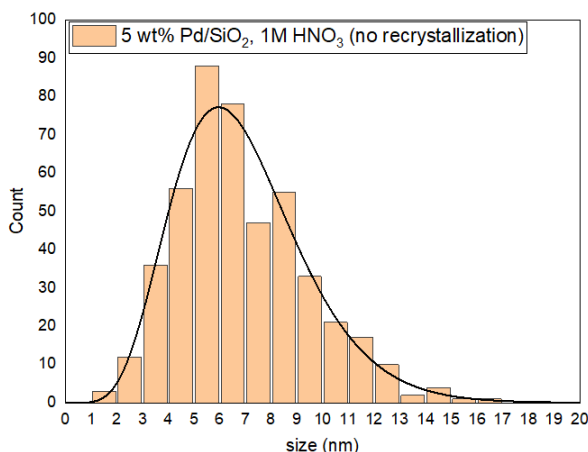


Figure 26: Size distribution of all the particles from 13 TEM images, except the two large chunks of Palladium from figure 25c and 25d, in the Pd/SiO₂ catalyst made with Pd(NO₃)₂ in 1M of nitric acid. Total number of particles counted is 464, with an average size of 6.89 nm and a standard deviation of 2.55 nm.

All the particles that are visible in the 14 images were counted, were considered inside the support, and that led to a total of 464 particles with an average size of 6.89 nm with a standard deviation of 2.55 nm. Significant amount of particles are larger than 10 nm, the diameter of the support. One of the explanations for this observance is that two particles overlap and are counted as one, which will lead to a higher average particle size. The diameter of the support could be divergent and larger than 10 nm, but on average the same as the theoretical value of 10 nm. As a result of these large particles and considering the pore sizes of the support, Palladium particles could have clogged up pores of the support leading to hindrance during catalytic testing. This will result in catalyst deactivation.

When the two large chunks of Palladium are taken in together with all the smaller particles, the results are the following: total number of particles that are counted are now 466, with an average size of 7.97 nm and a standard deviation of 18.2. So, the average size grew with 1.08 nm and the standard deviation is now over seven times larger than before. When the total volume of the particles was calculated, using the diameter and calculating the volume of a sphere with that diameter, the large particles in figure 13c and 13d hold over at least 99.5% of all the Palladium that has been found in the TEM images.

The chance that there are more large particles on other catalyst particles such as this one is high and therefore at least 99-99,9% of the Palladium metal is not inside the pores. This way, most of the metal does not contribute to activity of the catalyst as the surface to volume ratio is too small. With X-ray diffraction it is possible to compare the results for particle size obtained by TEM with the results calculated from diffraction patterns using the Sherrer equation.

These same results were also described by other studies. [61] Dann et al showed the difference between using a Palladium precursor solution with nitrates or using amines ($\text{Pd}(\text{NO}_3)_2$ and $\text{Pd}(\text{NH}_3)_4(\text{OH})_2$ on $\gamma\text{Al}_2\text{O}_3$). The difference is significant as 5% of the measured particles are larger than 15 nm for using nitrates and that is not observed for using amines, where an average diameter of 3.1 nm and a smaller size distribution is observed. For the nitrates Dann et al used a total molecular ratio of $\text{NO}^3/\text{Pd}=3.8$ for adding nitric acid. Other studies showed similar Palladium on Silica oxide particle sizes ranging from 5-13 nm. [42] So, the spread found by TEM on the catalyst is broader than theoretical values from literature, which were found by XRD as well as TEM.

4.6 X-ray diffraction

Next to analyzing the Palladium nitrate powder on purity, XRD can also be used to analyze the particle sizes. X-ray diffraction gives an indication for the particle size present in the catalyst. XRD diffraction patterns for calcined as well as calcined and reduced Palladium on silica catalysts on BASF support are being measured. It is expected to find Palladium oxide particles inside the support on calcined catalysts and Palladium metal particles on calcined and reduced catalysts. The calcined and reduced catalysts give a clear indication how large the catalyst particles are which are used during catalytic testing. Moreover, the sample tested on TEM can be compared to the results found with XRD.

The catalysts are measured on corresponding Palladium and Palladium oxide diffraction peaks. Between 37° and 57° Palladium oxide as well as the Palladium metal diffraction line has two corresponding peaks, see figure A2 and A3. At the conditions discussed in the experimental section the following XRD patterns are obtained for a calcined and a calcined and reduced catalyst, see figure 27. These XRD patterns are corrected for background as well as baseline in Origin resulting in the following, see figure 28.

Obtained XRD patterns without background and baseline correction

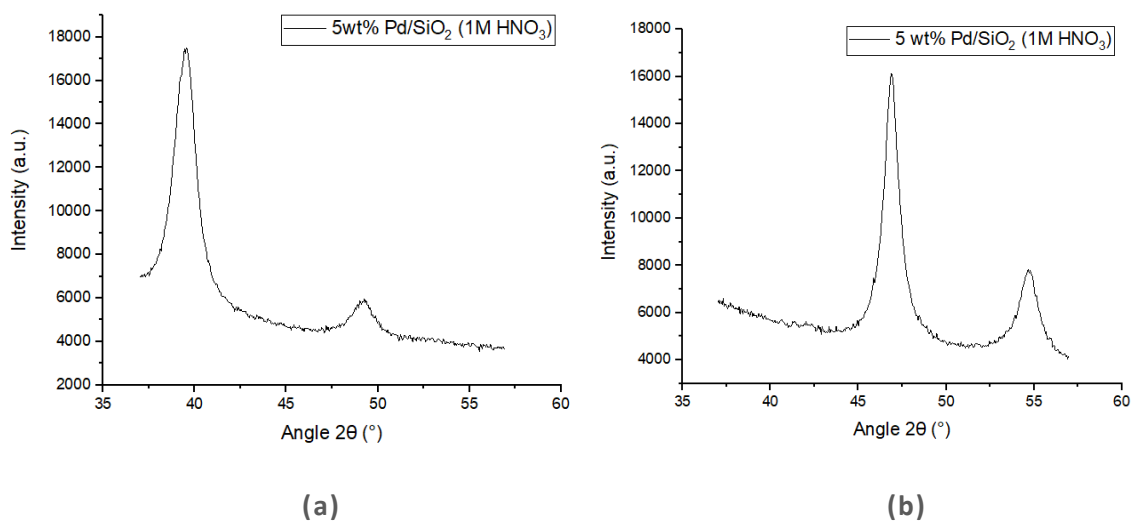


Figure 27. XRD diffractograms of 5 wt% Pd/SiO₂ catalysts, made by dissolving Pd(NO₃)₂ in 1M HNO₃ and general synthesis method. **a** Calcined catalyst and **b** calcined and reduced catalyst.

XRD patterns for PdO/SiO₂ and Pd/SiO₂

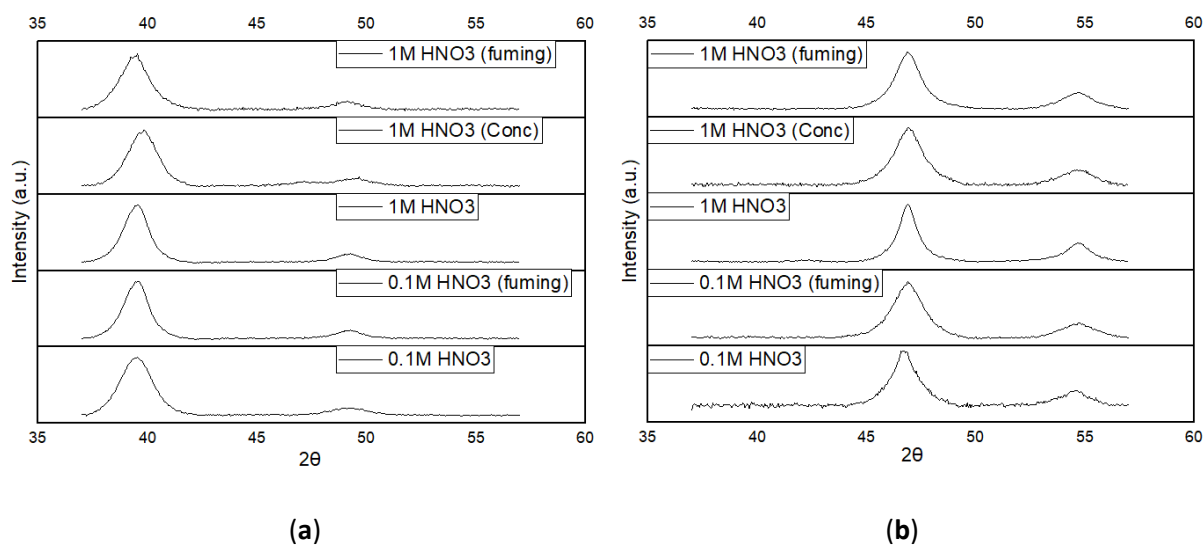


Figure 28. XRD patterns for **a** calcined and **b** calcined and reduced 5wt% Pd/SiO₂ catalyst on BASF-support corrected in Origin. Indicated in the figure is if normal Pd(NO₃)₂, recrystallized Pd(NO₃)₂ with fuming nitric acid or with concentrated nitric acid is used.

From these figures, with two different methods using the Sherrer equation in Origin as well as directly on the XRD pattern, is the particle size calculated, see figure 29. Per different recrystallization method is the average particle size given together with the standard deviation for the calcined catalysts as well as the reduced catalysts.

In the diffraction patterns peak shifts as well as different forms of peaks can be assigned. A broader peak indicates a smaller particle size, as follows from the Scherrer equation in equation 12. Assigning a broad peak could be difficult, especially because the second peak, the rightmost peak, is already lower in intensity than the left one. The program, which uses the Scherrer equation directly on the diffractogram, finds it difficult to divorce a peak from the noise level. Therefore, it was not always possible to measure the second peak using two methods. The method using Origin always resulted in a value for β . In some cases, the particle size as well as the standard deviation was only the result of three averaged peaks instead of four.

Average Palladium Particle sizes from XRD on BASF support

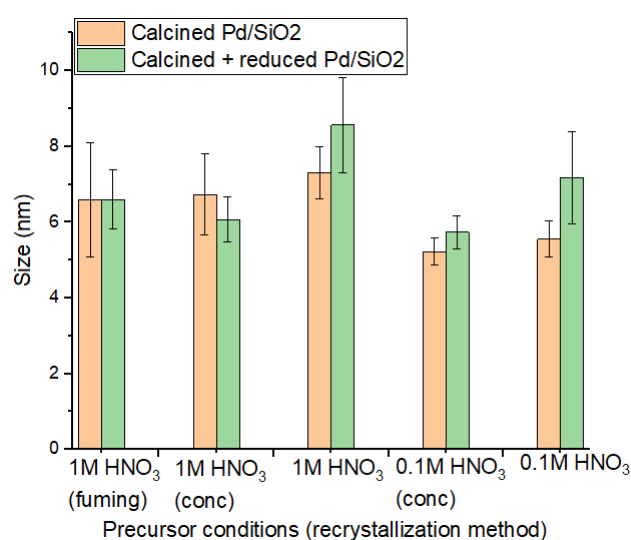


Figure 29. Average particle size calculated by the Scherrer equation and the XRD spectra from figure 28 with two different methods. Error bars indicate the standard deviation over the four (sometimes three) calculated/measured particle sizes.

From the results in figure 29 it is found that the recrystallization, for fuming as well as concentrated nitric acid recrystallization agent, gives a smaller particle size, in the calcined as well as calcined and reduced catalyst, than using a non-recrystallized precursor salt. The difference between the two different recrystallization methods at 1M of nitric acid is small (0.5 nm) but still reasonable. It was expected that using a precursor solution with less Palladium (oxide) metal this would lead to lower particle sizes as the change on sintering becomes significantly lower. This is not observed from the XRD results between the two different recrystallization methods and the Palladium nitrate purity they represent, where the differences were quite large. Therefore, the purity of Palladium nitrate does not play a significant role in the Palladium particle size in the support and an opposite result is observed. The small difference can still come from the stability of the precursor solution, as not every parameter can be kept exactly the same, which is certainly the case for the impregnation step.

Between the recrystallized and non-recrystallized Palladium nitrate catalyst at 0.1M of nitric acid the same differences are observed as at 1M of nitric acid in precursor solution. With an average size of 5.7 nm the fuming Palladium nitrate catalyst has a significantly smaller particle size than the non-recrystallized at 7.2 nm for a final reduced catalyst.

Then the TEM results discussed earlier are compared with the XRD results discussed above. The catalysts discussed in TEM consisted of non-recrystallized calcined and reduced Palladium on the BASF support in 1M of nitric acid precursor conditions. This resulted in an average particle size of 7.97 nm and without the two large sintered Palladium particles the average particle size was 6.89 nm. The same catalyst in XRD showed an average particle size of 8.56 nm with a standard deviation of 1.25 nm. The TEM result of all the particles, the 7.97 nm, falls in the standard deviation of the XRD result and could therefore be possible. As expected, there will be more larger particles found in TEM as has been characterized, which will increase the average particle size. So, the XRD gives indeed an indication for the particle size compared to the TEM result.

Besides the Palladium on BASF-silica catalyst there were also some Palladium catalysts synthesized on CARiACT-silica. These catalysts were analyzed the same way as the BASF catalysts, see figure 30. For this kind of catalyst, the precursor solution was made with a different Palladium nitrate salt as the other catalysts on the BASF-silica support. Moreover, a catalyst was made with Palladium dissolved in concentrated nitric acid (15.6M) which resulted in the smallest particle sizes of all the catalysts, for the calcined and reduced catalysts. The smallest calcined catalyst is at 0.1M of nitric acid. This is interesting, as the reducing reaction has a large increase in particle size as a result. From 5.47 to 8.75 nm and even the standard deviation is increasing largely. This catalyst is the only catalyst where the standard deviation between the calcined and the calcined and reduced catalyst carry out not to overlap, even at a large standard deviation. Showing the significant increase in particle size.

Average Palladium particle sizes from XRD on CARiACT support

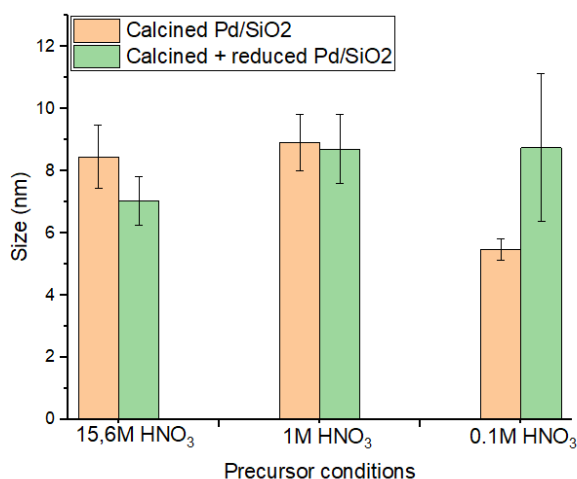


Figure 30. Average particle size calculated with the Scherrer equation for CARiACT support with non-recrystallized Pd(NO₃)₂ with two different methods. Error bars indicate the standard deviation over the four calculated/measured particle sizes.

When the different concentrations of Palladium sources are compared the following conclusions can be taken. The BASF 1.0M nitric acid non-recrystallized and the CARiACT 1.0M non-recrystallized catalysts both contained the 39% Palladium nitrate source and were only different for two reasons. The difference in particle size is 7.31 and 8.57 nm for the BASF and 8.90 and 8.71 nm for the CARiACT for the calcined and reduced respectively. Apart from the different support the catalyst was treated with cooled precursor conditions to enhance stability. For the 0.1M nitric acid precursor conditions the results were as follows: 5.56 and 7.18 nm for BASF and 5.47 and 8.75 nm for the CARiACT for the calcined and reduced respectively. This time the precursor solution consisted of a mixture of the 39% and 41% Palladium nitrate for the BASF support and no difference was made in precursor conditions. The result showed a similar effect going from calcined to reduced catalyst. The calcined catalysts contained similar sizes but reducing the catalysts resulted in a larger sintering for the CARiACT catalyst. This difference between the catalysts can only be explained as the mixture of the 39% and 41% Palladium nitrate and can't be the result of a different support, as it was already shown that the support does not lead to significant changes.

4.7 Operando infrared radiation

In the last part of the results and discussion section the catalytic ability of some of the synthesized catalysts were tested, mainly to determine the benefit of having a stable precursor solution consisting of purer Palladium nitrate. If the catalyst, containing the fuming nitric acid recrystallized Palladium nitrate, shows a higher activity towards a certain reaction, than the catalyst containing the non-recrystallized Palladium nitrate, this could be the result of improved precursor conditions. Yet, this is depending on several other parameters than the purity of Palladium nitrate:

- The catalyzed reaction. This matters because the characterization of the catalysts nanoparticles determines the activity towards a reaction depending on what kind of reaction it is, as well as the reactants used. As described before, hydrogenation reactions are the key reaction for the Nickel-Palladium bimetallic catalysts. CO₂ and H₂ are used as reactants and the amount of produced methane is measured. For monometallic Palladium catalysts, it is expected that the activity towards this reaction is not high because Nickel is a key component in this reaction. Though, it could give valuable information comparable to the Palladium catalysts.
- The amount of metal in the catalysts. In theory the more metal nanoparticles are dispersed, having the same diameter, the higher the catalytic activity due to more active centra. Having too large amount of metal can block pores and makes sintering a serious problem.
- The particle sizes. From XRD are the average particle sizes known and this will also influence the catalytic activity of the catalysts. Smaller particles have in theory a higher surface to volume ratio, hence beneficial structural and electronic aspects. [62]

The rest of the parameters were expected constant and in the same conditions, making differences in activity directly an effect from differences in precursor conditions and the consequence of that on particle sizes. From there, conclusions will lead to knowledge on CO₂ hydrogenation of Palladium.

The activity of different catalysts was tested on a DRIFTS cell and analyzed by IR measurements. A drift cell was used due to failure of the original cell. Therefore, a limited amount of catalyst were possible to test and the results show limited data points, due to shorter measurement time. The tested catalysts contained multiple different parameters to utilize the limited amount of tests. From the discussion the origin of the change in activity can be determined and follow up experiments can be developed.

The three catalysts tested are all consisting of BASF support and contain precursor conditions: (percentage values of metal weight are obtained from ICP-OES)

- 5.6 wt% non-recrystallized Palladium nitrate (39.1%) in 1M of nitric acid
- 3.5 wt% fuming nitric acid recrystallized Palladium nitrate (41%) in 1M of nitric acid
- 5.0 wt% fuming nitric acid recrystallized Palladium nitrate (41%) in 0.1M of nitric acid

The results of these catalysts are obtained and together with a calibration line for CO₂ as well as for methane, the amount of formed methane is calculated, see figure 31a. The amount of CO₂ consumed was also determined but not shown in the figure. Because it was difficult for DRIFTS to use the exact same amount of catalysts for each measurement the results were adapted for the amount of catalyst used as well as the amount of Palladium loaded on the Silica support, see figure 31b.

Formation of methane by catalytic reaction of CO₂ and H₂ of three different Pd/SiO₂ catalysts differing by precursor conditions.

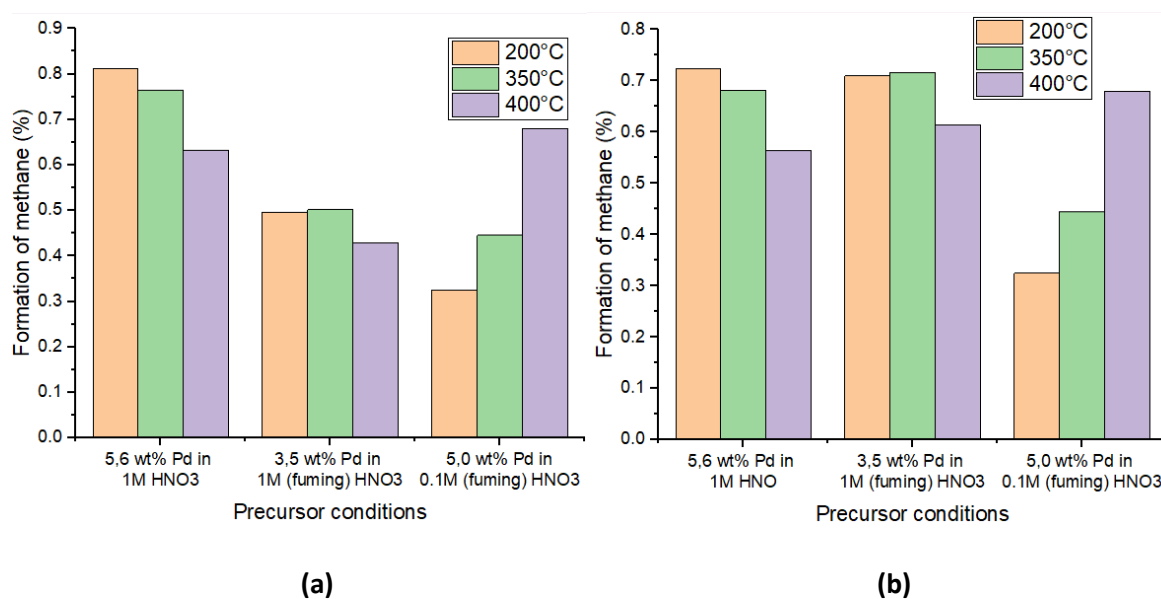


Figure 31. The amount of methane produced from CO₂. The percentages on the y-axis indicate the amount of methane produced compared to the maximum amount when all CO₂ is converted to methane. **a** Shows the amount of methane formed during catalytic testing and **b** shows the amount of methane formed per 20 mg of catalyst and 5.0 wt% of Palladium.

The results, obtained from figure 31, show similar formation of methane per moles of Palladium metal for the non-recrystallized Palladium nitrate catalysts at 1.0M nitric acid as the recrystallized Palladium nitrate using fuming nitric acid catalyst at 1.0M nitric acid. Using fuming nitric acid as a recrystallization agent shows slightly higher production at higher temperature (350°C and 400°C) than the non-

recrystallized catalyst. Moreover, these results show high formation of methane at low temperature (200°C) and lower at higher temperature (400°C). The opposite effect is observed for the catalysts consisting of the recrystallized Palladium nitrate (using fuming nitric acid) catalysts in 0.1M nitric acid precursor conditions. The highest methane formation at 400°C is observed for these catalysts, close to the maximum formation at lower temperatures of non-recrystallized catalysts. The exact amount of methane produced per second per moles of Palladium gives the turn-over frequency (TOF), see figure 32.

TOF of CO₂ methanation by Pd/SiO₂ catalysts consisting of three different precursor conditions.

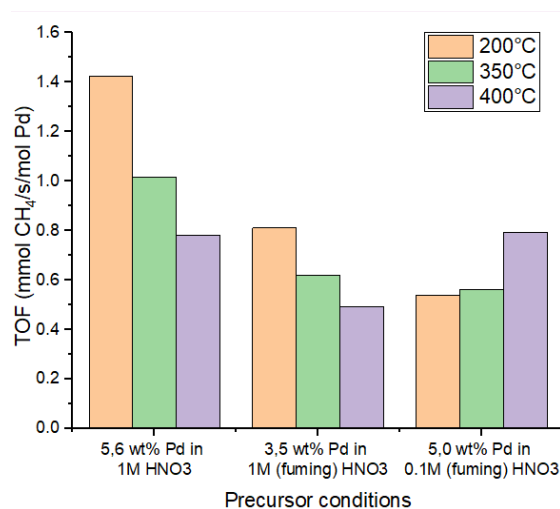


Figure 32. Turn-over frequency on CO₂ methanation towards CH₄ of three different Pd/SiO₂ catalysts consisting of different precursor conditions: non-recrystallized Palladium nitrate at 1M of nitric acid and recrystallized Palladium nitrate at 1M and 0.1M of nitric acid.

This makes the non-recrystallized Palladium nitrate at 1.0M nitric acid catalyst preferable at low temperatures and the recrystallized fuming nitric acid Palladium nitrate at 0.1M of nitric acid at higher temperatures appealing. The difference between the two catalysts, containing the recrystallized Palladium nitrate, is not large and therefore the benefit of using milder conditions outweighs the marginal change in TOF. This makes the catalysts containing the recrystallized Palladium nitrate still a promising catalyst from operando data.

Considered here are the different Palladium nitrate sources used for the tested catalysts. As was stated before the 39% Palladium nitrate was more stable in UV-vis. Therefore, it was expected that the non-recrystallized catalyst would be a more stable catalyst, which could result in higher methane formation. If a non-recrystallized catalyst, consisting of the more unstable 41% Palladium nitrate, results in a

significantly less formation of methane is unknown due to the limited amount of tests possible. But was expected due to the large difference in instability. As a result, the catalysts containing recrystallized Palladium nitrate from fuming nitric acid could indeed lead to higher affinity towards methane but this is not the case because of this. It was expected that the 41% recrystallized Palladium nitrate would be significantly better than the non-recrystallized Palladium nitrate, independently of the Palladium source that is used. The results are too limited to conclude these assumptions.

Literature showed that relatively large Palladium particles promote more the activity of CO hydrogenation and fine particles of around 2 nm more on ethane hydroformylation. [42] If the CO hydrogenation can be assumed to have similar results as for CO₂ hydrogenation the results obtained shows indeed that larger particles, in the 5.6 wt% catalysts, has higher activity towards methane as smaller particles. Therefore, smaller average sizes of Palladium particles does not contribute to higher methane formation, as expected. Considering the similar activity towards methane of the analyzed catalyst could indicate that the same particle sizes have been found, but less sintering outside the support. But this is an assumption. TEM could clarify if this is the case.

5. Conclusion

For improving Nickel supported catalysts, often used in hydrogenation reactions, addition of a noble metal in the form of Palladium was considered. Using Palladium as a bimetallic component together with Nickel has several benefits as a supported hydrogenation catalyst, especially in bimetallic alloy. Making Palladium useful for bimetallic catalysts is easy when using a precursor solution with stable Palladium salts, such as Palladium chlorides. Unfortunately, some of the salt will remain in the catalyst after synthesis and will lead to performance inhibition and deactivation of the catalyst. These potential inhibitors will deactivate the catalyst performing even worse than a monometallic Nickel catalyst on the designed catalytic reaction. Palladium nitrate could potentially lead to increased catalytic activity, but this was not the case as was shown by previous research done in the Inorganic Chemistry and Catalysis group (not published).

The subject of this thesis was to make Palladium nitrate more universal applicable as a viable option in precursor solutions for (bi)metallic catalysts. From experiments it was clear that the quality of available Palladium nitrate sources diverge and contain impurities in the form of solid (chunks) Palladium oxide, leading to rapid formation of particles in solution. The thesis describes the process of Palladium nitrate improved to a workable precursor solution by recrystallizing Palladium nitrate. Further, the influence of the recrystallization on the performance of the salt in catalysts is discussed. From here, optimization of the stable Palladium nitrate can be used to find stable conditions for bimetallic catalyst synthesis.

Effect of recrystallization of Palladium nitrate on purity and precursor stability

Palladium nitrate was successfully recrystallized using fuming nitric acid as a recrystallization agent by distillation of pure nitric acid and vacuum evaporation/crystallization. The purity of the (41%) Palladium nitrate as well as the stability in solution improved substantially, concluded from XRD and UV-vis experiments. Considering full drying of the recrystallized Palladium nitrate with fuming nitric acid, the newly obtained Palladium nitrate contained 40.7% Palladium, where the original Palladium nitrate source contained 41% Palladium, analyzed by ICP-OES. Therefore, the new coordination for the

salt is $\text{Pd}(\text{NO}_3)_2 \cdot 1.73 \text{ H}_2\text{O}$, where the original source contained 1.62 water molecules per Palladium nitrate molecule. This Palladium nitrate in low nitric acid concentrations precursor solution resulted in an increased stability at different concentrations of nitric acid compared to the original (more stable than the 41%) 39% Palladium nitrate, measured by UV-vis.

Using concentrated nitric acid as a recrystallization agent, resulted in less successful recrystallization and less stable precursor solution compared to the recrystallized Palladium nitrate obtained from using fuming nitric acid. The XRD pattern showed this performance as well, the XRD pattern was in most conformity towards the original non-recrystallized 41% Palladium nitrate source. From ICP-OES analysis the newly recrystallized Palladium nitrate contained 35.3% Palladium. The salt structure corresponding to this Palladium percentage is unlikely, as Palladium nitrate forms a square planar complex where only a limited amount of water molecules could be around the salt. [32] Presumably, using concentrated nitric acid as a recrystallization agent results in less dry Palladium nitrate salt. Longer vacuum drying is needed to remove the water from the powder.

The recrystallized Palladium nitrate with fuming nitric acid showed more than twice the amount of stability in terms of formation of Palladium oxide than the non-recrystallized precursor (39%) in 0.1M of nitric acid, which was already considered the more stable non-recrystallized Palladium nitrate. The recrystallized Palladium nitrate by concentrated nitric acid resulted in less stability than the non-recrystallized Palladium nitrate; almost twice the amount of Palladium oxide is formed than the 39% Palladium salt in 0.1M of nitric acid. The stability of 41% was not tested due to high/fast formation of Palladium oxide, making this precursor solution the most unstable solution.

Effect of recrystallization of Palladium nitrate on particle sizes and catalytic activity

Both the recrystallized Palladium nitrate salts synthesized on Silica support resulted in smaller particle sizes compared with the non-recrystallized catalyst made with the older (and more stable 39%) Palladium nitrate consisting of $8.6 \pm 1.3 \text{ nm}$ at 1M and 7.2 ± 1.21 at 0.1M of nitric acid. On the BASF support the particle sizes are on average $6.6 \pm 0.8 \text{ nm}$ and $5.7 \pm 0.4 \text{ nm}$ at 0.1M at 1.0M of nitric acid. Using nitric acid as a recrystallization agent resulted in particle sizes of $6.1 \pm 0.6 \text{ nm}$ at 1.0M of nitric acid. As a result, the surface to volume ratio of the particle sizes increases, relative to using the 39% Palladium nitrate, which resulted in higher reactivity of the catalyst on the metal surface atoms. This makes the catalyst in theory more active towards hydrogenation reactions.

Results of operando IR shows similar formation of methane for the non-recrystallized 39% Palladium nitrate as for the recrystallized fuming nitric acid Palladium nitrate from the 41% source. At 0.1M of nitric acid, thus milder precursor conditions, using recrystallized Palladium nitrate resulted in an opposite effect than the 39% Palladium, resulting in increased methane formation at increasing

temperatures. At 400°C similar methane formation was obtained as for the non-recrystallized Palladium catalyst, making a recrystallized Palladium nitrate catalysts at 0.1M of nitric acid as well as the non-recrystallized Palladium nitrate catalyst at 1.0M of nitric acid. This makes the recrystallized Palladium catalyst favorable over the non-recrystallized catalyst due to the milder precursor conditions. This method results in making a comparable catalyst to the 39% Palladium catalyst, but a broader research is necessary.

It can be concluded, using concentrated (68%) nitric acid to recrystallize Palladium nitrate resulted in a powder that was not dry enough and resulted in little increased stability. This makes concentrated nitric acid not an efficient method for making Palladium nitrate a viable option. Contrary to this, using fuming nitric acid as a recrystallisation agent resulted in highly improved Palladium nitrate compared to the 41% Palladium nitrate source in different ways. Yet, further improvement is possible with this method making Palladium nitrate a reliable option for bimetallic catalysts.

Bimetallic precursor stability

To conclude this thesis, there has been a first step towards bimetallic precursor solution stability using the 39% "reasonable" stable Palladium nitrate. The optimal concentration of nitric acid at a total of 5 wt% metal and 90:10 Ni:Pd ratio was analyzed. The next step is the design of the bimetallic catalyst. The influence of Palladium ions and Nickel ions in different conditions was measured with UV-vis. It was concluded that the optimal concentration for the bimetallic precursor solution in nitric acid, showing the lowest particle formation, is at 2M of nitric acid, being the concentration of the solution and not the concentration of nitric acid added to the two salts.

6. Outlook

This section of the thesis sums up the possible improvements that can be obtained on this research. What kind of research is needed in reaching reliable and consistent Palladium nitrate solutions contributing to improvements on bimetallic catalysts. The results summed up in the conclusion shows further improvements by enhancing aspects, which could be on the Palladium nitrate salt, precursor solution and on catalysts level. In this section suggestions are made for future experiments that can lead to interesting properties or activities for monometallic as well as bimetallic Palladium catalysts.

Improving the purity of Palladium nitrate

From the results and observing the salt, it was clear that different qualities of Palladium nitrate are on the market ranging between percentage of Palladium and Palladium nitrate purity. By using different qualities of Palladium nitrate the effectiveness of fuming nitric acid as a recrystallization agent was demonstrated. Improvements on the recrystallization method can lead to full Palladium nitrate purity and full removal of Palladium (oxide). Performing the recrystallization twice on the same salt could be sufficient, as the amount of water generated by removing Palladium oxide also lowers the strength of the solution. It has to be investigated if this is the case. The amount of Palladium oxide that remains has to be measured to quantify the effectiveness. UV-vis is not the best method for this and XRD in combination with Rietveld analysis could result in a more quantitative result.

Literature showed that solutions containing around 20 wt% of Palladium can be stored for longer periods to indefinitely when the ratio of free nitric acid and Palladium ions is no less than 1:1 and concentration of nitric acid is not lower than 3M. [63] When these conditions are met this may result in an improved Palladium nitrate precursor solutions as well.

Other options to reach higher purity, besides doing multiple recrystallizations on the same salt, is using more fuming nitric acid. Synthesizing fuming nitric acid is labor intensive, as the reaction needs to be supervised (if it is still running or running too hard this will result in lower concentration of nitric acid). Using concentrated nitric acid as a first recrystallization method could already save time and money.

But only using concentrated nitric acid will not be sufficient to get rid of all the Palladium oxide as almost a third is water. Downside of this method could be that a significant amount of water is left in the Palladium nitrate powder. This remaining water will decrease the concentration of fuming nitric acid the next time Palladium nitrate recrystallization is performed.

Other ways to improve the precursor salt could be to turn the available Palladium oxide into solid Palladium metal by a redox reactions. Afterwards, it is easier to turn solid Palladium back into Palladium nitrate than from Palladium oxide.

Finally, it is important to dry the recrystallized Palladium nitrate longer than is performed now. The difficulty is that only a static vacuum could be applied when the salt is dried for a longer time, because safety steps are needed when using the pump. This to prevent acidic gases and water to damage the pump and releasing toxic gases to exit into the air. This set-up freezes the evaporated nitric acid. In theory, after the salt is sufficiently dry a vacuum pump can be used with a solid acidic trap consisting of Sodium hydroxide powder instead of tablets.

It could be important to reach full purity towards Palladium nitrate. The speed of particle formation and growth decreases at lower concentration of Palladium (oxide) particles, as was shown. A powder containing no Palladium (oxide) particles could result in (significant) slow formation of particles at mild/neutral conditions. Results of these mild stable precursor conditions have large benefits over using acidic conditions and could favor binding to the support.

Did any more sintering take place on the support?

This is one the of the most important aspects towards using Palladium nitrate as Palladium needs to be used efficient inside the pores. It was shown that even the more stable considered 39% Palladium nitrate was affected by large sintering of Palladium. The less stable regarded 41% Palladium nitrate was not imaged in TEM as well as the catalysts containing the recrystallized Palladium nitrate, due to moving the device to another building. This is unfortunate and would have given a large contribution to this thesis.

As the TEM of the non-recrystallized (39%) Palladium nitrate gave a broad particle sizes, even particles larger than the pore sizes, as compared obtained from XRD, it gives an indication that as the average particle size for the recrystallized Palladium catalysts is smaller the change on large sintering on the support could be smaller. But again, this is an indication and more TEM on the catalyst should give more exclusion. Moreover, also the difference on sintering between 0.1M and 1.0M of nitric acid in the precursor conditions can be analyzed. When on both catalysts no more large sintered particles are found, or significantly smaller or less, it supports this research into using Palladium nitrates. A larger

percentage of the Palladium is then inside the pores contributing to higher production of certain designed reaction products.

When analyzing the tested catalysts by TEM the particle sizes can be analyzed in more detail. This way, the assumption indicating that smaller found particle size by XRD and similar catalytic activity is the result of less sintering outside the support reaching similar particle sizes for all catalysts.

More future research onto Palladium nitrate stability

When new Palladium nitrate is recrystallized with a higher purity, or even full purity, it is interesting to what extent a precursor solution can be maintained stable. Till now, Palladium nitrate in water is unstable as direct formation of Palladium (oxide) particles is observed. If a solution with stable Palladium ions in water or a low acidic solution is designed, that would be a great step into useful conditions of the catalyst.

Next step on bimetallic catalysts

In the end, the most important item is that Palladium nitrate works for bimetallic synthesis. This was not yet tested in the form of catalysts, therefore the next step after having a (more) stable salt is finding the optimal conditions for bimetallic synthesis. This must then improve the catalytic activity to a certain reaction, which was not the case as Palladium had as an effect to decrease the methane formation in relation to a monometallic Nickel catalyst. Some conditions to adapt are summarized below:

1. The precursor conditions could be different. The precursor conditions were now checked for 5 wt% 90:10 ratio of Nickel and Palladium and were optimal at a concentration of 2M nitric acid. For a different stability of Palladium, the optimal concentration for nitric acid could be different. The same can be said for different ratios of Nickel and Palladium, as well as for different total metal weights used.
2. The drying stage can be optimized by freeze drying or even by using precursor solutions in colder conditions that will decrease the rate of particle formation. [37]
3. The total metal percentage can be optimized. Not only the total metal weight, which was till now 5 wt%, but also the ratio between Nickel and Palladium can be changed. This could lead to different alloys. The Palladium catalyst analyzed in TEM showed filled pores and yet most of the Palladium was found outside the support. Therefore, even lower weight percentages could lead to similar results. This was also shown in the catalytic activity part of the results section.
4. Calcination and reduction temperatures are now designed for the conditions above but could also change due to differences in alloys. Therefore, TPR or Thermogravimetric Analysis by Mass Spectrometry (TGA-MS) can be used to analyze the newly synthesized compounds.

Every single step towards a better catalyst can be tested for hydrogenation by CO₂ methanation. A systematic study could lead to optimal conditions. This was not interesting for the Palladium catalysts as this may largely differ to a bimetallic catalyst.

Other useful catalysis reactions

As this catalyst is useful for not only CO₂ hydrogenation, but it could be useful towards other hydrogenation reactions. The Nickel-Palladium on Silica oxide support is not only limited to catalyzing hydrogenation reactions, [64] as it theoretically can be used for hydrodeoxygenation reactions. More articles are written about using these kinds of catalysts for hydrodeoxygenation reactions than for CO₂ hydrogenation.

One important field for future use of hydrogenation catalysts is the utilization of biomass, as biomass in certain forms has lots of potential when it comes to reuse instead of burning it. For example, a product from biomass is furfural. The Pd/SiO₂ catalyst is already investigated for the use in furfural hydrogenation. [65] The bimetallic catalyst containing Nickel and Palladium could lead to improved product synthesis.

Another interesting product of biomass is the compound guaiacol. This organic compound is not yet useful as a reactant and is therefore largely burned. For making useful products such as benzene and phenol out of guaiacol a catalyst is needed that has large pores, accessible for the large guaiacol molecule, and active towards hydrodeoxygenation reactions, by noble metals, [66] [67] also performed by the ICC group. [68] Similar catalysts or even overlayer catalysts are used for these kinds of reactions. [69]

7. Acknowledgements

I would like to thank Florian Zand for the daily supervision and help with the project. This project was done during Covid times, which made it sometimes challenging to obtain together and discuss the project. Many thanks for making time for me during these difficult times. I have learned a lot on synthesizing catalysts with incipient wetness impregnation methods and on being critical of my research. I guess it was not the best period to join the Inorganic Chemistry and Catalysis group, but I liked most of the time I was there. Especially, the last months that I worked on recrystallization.

During the times that Florian was not available to supervise me, Kordula Schnabl helped me progress my research. Also, I could use her set-up for drying my catalysts. Thanks for that and the helpful discussions.

Furthermore, thanks to Ward van der Stam for the discussions on how to progress with the project and to improve my qualities. Dannie Wezendonk for helping me work with XRD. Jochem Wijten for designing safe set-ups with me. Coen Mulder for ICP-OES data. Luc Smulders for the training on the QuadCal and lastly Luke Parker for helping me on UV-vis.

8. Bibliography

- [1] C. Song, S. Park and J. Shin, "Tropical Cyclone Activities in Warm Climate with Quadrupled CO₂ Concentration Simulated by a New General Circulation Model," *Journal of Geophysical Research*, vol. 125, pp. 1-14, 2020.
- [2] V. Masson-Delmotte, H. Portner, J. Skea, P. Zhai, D. Roberts, P. Shukla, A. Pirani, W. Moufouma-Okia, C. Pean, R. Pidcock, S. Connors, J. R. Matthews, Y. Chen, X. Zhou, M. Gomis, E. Lonnoy, T. Maycock, M. Tignot and T. Waterfield, "Global Warming of 1.5°C An IPCC Special Report on the impacts of global warming of 1.5°C above pre-industrial levels and," *IPCC*, pp. 1-630, 2018.
- [3] "Climate Central," 15 January 2020. [Online]. Available: <https://www.climatecentral.org/gallery/graphics/top-10-warmest-years-on-record>.
- [4] N. Golledge, "Long-term projections of sea-level rise from ice sheets," *Wiley Interdisciplinary Reviews*, vol. 11, no. 2, p. 21, 2019.
- [5] P. Tans, J. Shakun, G. Dutton and E. Dlugokencky, "Global CO₂ Levels," 2 Degrees Institute, [Online]. Available: <https://www.co2levels.org/>. [Accessed 8 August 2021].
- [6] "EPA," 27 July 2021. [Online]. Available: <https://www.epa.gov/ghgemissions/overview-greenhouse-gases>.
- [7] T. Anderson, E. Hawkins and P. Jones, "CO₂, the greenhouse effect and global warming: from the pioneering work of Arrhenius and Callendar to today's Earth System Models," *Endeavour*, pp. Vol 40 No.3 178-187, 2016.
- [8] D. E. Authority, "Voortgang Emissiehandel 2019," Den Haag, 2019, p. 35.

- [9] L. Wisse, "NOS," 10 August 2021. [Online]. Available: <https://nos.nl/artikel/2393412-klimatetrapport-leidt-niet-tot-spoedvergaderingen-in-bestuurskamers>.
- [10] R. Z, "RTL Nieuws," 9 August 2021. [Online]. Available: <https://www.rtlnieuws.nl/economie/artikel/5247243/grootste-vervuilers-nederland-co2-uitstoot-ippc-shell-tata>.
- [11] U. Nations, "UNFCCC," 2015. [Online]. Available: https://unfccc.int/sites/default/files/english_paris_agreement.pdf. [Accessed 20 August 2021].
- [12] J. Sinfelt, "Bimetallic Catalysts," *Scientific American*, vol. 253, no. 3, pp. 90-101, 1985.
- [13] H. Davy, "VIII. Some new experiments and observations on the combustion of gaseous mixtures, with an account of a method of preserving a continued light in mixtures of inflammable gases and air without flame," *Philosophical Transactions of the Royal Society of London*, vol. 107, pp. 77-85, 1817.
- [14] P. Munnik, P. E. d. Jongh and K. d. Jong, "Recent Developments in the Synthesis of Supported Catalysts," *Chemical Reviews*, pp. 6687-6718, 2015.
- [15] G. Borekov, *Heterogeneous Catalysis*, New York: Nova Science Publishers, Inc, 2003.
- [16] M. Sankar, N. Dimitratos, P. Miedziak, P. Wells, C. Kiely and G. Hutchings, "Designing bimetallic catalysts for a green and sustainable future," *Chemical Society Reviews*, vol. 41, pp. 8099-8139, 2021.
- [17] F. Pompeo, N. Nichio, O. Ferretti and D. Resasco, "Study of Ni catalysts on different supports to obtain synthesis gas," *International Journal of Hydrogen Energy*, vol. 30, no. 13-14, pp. 1399-1405, 2005.
- [18] D. Deng, H. Guo, B. Ji, W. Wang, L. Ma and D. Luo, "Size-selective catalysts in five functionalized porous coordination polymers with unsaturated zinc centers," *New Journal of Chemistry*, vol. 41, pp. 12611-12616, 2017.
- [19] R. Mu, Q. Fu, H. Xu, H. Zhang, Y. Hang, Z. Jiang, S. Zhang, D. Tan and X. Boa, "Synergetic Effect of Surface and Subsurface Ni Species at Pt-Ni Bimetallic Catalysts for CO Oxidation," *Journal of the American Chemical Society*, vol. 133, pp. 1978-1986, 2011.
- [20] R. Huang, Y. Wen, Z. Zhu and S. Sun, "Pt-Pd Bimetallic Catalysts: Structural and Thermal Stabilities of Core-Shell and Alloyed Nanoparticles," *The Journal of Physical Chemistry C*, vol. 116, pp. 8664-8671, 2012.

- [21] J. Martinez, E. Hernandez, S. Alfaro, R. Medina, G. Aguilar, E. Albiter and M. Valenzuela, "High Selectivity and Stability of Nickel Catalysts for CO₂ Methanation: Support Effects," *Catalysts*, vol. 9, no. 24, p. 13, 2019.
- [22] W. Wang, S. Wang, X. Ma and J. Gong, "Recent advances in catalytic hydrogenation of carbon dioxide," *Chem Soc Rev*, vol. 40, pp. 3703-3727, 2011.
- [23] P. Munnik, M. Velthoen, P. D. Jongh, K. D. Jong and C. Gommers, "Nanoparticle Growth in Supported Nickel Catalysts during," *Angew. Chem.*, vol. 126, pp. 9647-9651, 2014.
- [24] K. Ghaib and F. Ben-Fares, "Power-to-Methane: A state-of-the-art review," *Renewable and Sustainable Energy Reviews*, vol. 81, pp. 433-446, 2018.
- [25] W. Shen, M. Okumura, Y. Matsumura and M. Haruta, "The influence of the support on the activity and selectivity of Pd in CO hydrogenation," *Applied Catalysis A: General*, vol. 213, pp. 225-232, 2001.
- [26] W. Shen, A. Kobayashi, Y. Ichihashi, Y. Matsumura and M. Haruta, "Growth of Pd particles in methanol synthesis over Pd/CeO₂," *Catalysis Letters*, vol. 73, no. 2-4, pp. 161-166, 2001.
- [27] N. Bion, F. Epron, M. Moreno, F. Marino and D. Duprez, "Preferential Oxidation of Carbon Monoxide in the Presence of Hydrogen (PROX) over Noble Metals and Transition Metal Oxides: Advantages and Drawbacks," *Top Catalysis*, vol. 51, pp. 76-88, 2008.
- [28] O. Pozdnyakova, D. Teschner, A. Wootscha, J. Kröhnert, B. Steinhauer, H. Sauer, L. Toth, F. Jentoft, A. Knop-Gerick, Z. Paál and R. Schlögl, "Preferential CO oxidation in hydrogen (PROX) on ceria-supported catalysts, part II: Oxidation states and surface species on Pd/CeO₂ under reaction conditions, suggested reaction mechanism," *Journal of Catalysis*, vol. 237, no. 1, pp. 17-28, 2006.
- [29] T. Eggenhuisen, J. Zecevic, H. Talsma, K. d. Jong and P. d. Jongh, "Quantitative Assessment of Pore Blockage in Supported Catalysts: Comparing Differential Scanning Calorimetry and Physisorption," *The Journal of Physical Chemistry*, vol. 116, no. 13, pp. 7480-7490, 2012.
- [30] T. Eggenhuisen, M. Steenbergen, H. Talsma, P. d. Jongh and K. d. Jong, "Impregnation of Mesoporous Silica for Catalyst Preparation Studied with Differential Scanning Calorimetry," *The Journal of Physical Chemistry*, vol. 113, no. 38, pp. 16785-16791, 2009.
- [31] C. d. M. Donegá, *Nanoparticles Workhorses of Nanoscience*, Utrecht, The Netherlands: Springer, 2014.

- [32] M. Toebes, J. Dillen and K. Jong, "Synthesis of supported palladium catalysts," *Journal of Molecular Catalysis A: Chemical* 173, pp. 75-98, 2001.
- [33] J. Brunelle, "Preparation of Catalysts by Metallic Complex Adsorption on Mineral Oxides," *Pure & Appl. Chem.*, pp. 1211-1229, 1978.
- [34] M. Wolters, L. v. Grotel, T. Eggenhuisen, J. Sietsma, K. d. Jong and P. d. Jongh, "Combining confinement and NO calcination to arrive at highly dispersed supported nickel and cobalt oxide catalysts with a tunable particle size," *Catalysis Today*, vol. 163, pp. 27-32, 2011.
- [35] "Fuji Silysia Chemicals LTD," 2013. [Online]. Available: <https://www.fujisilysia.com/products/cariact/>.
- [36] BASF, "Perlkat 97-0 Silica Gel," may 2019. [Online]. Available: https://catalysts.basf.com/files/literature-library/BASF_Perlkat-97-0-Silica-Gel_Datasheet_Rev.-2019-05_A4.pdf.
- [37] T. Eggenhuisen, H. Friedrich, F. Nudelman, J. Zecevic, N. Sommerdijk, P. d. Jongh and K. d. Jong, "Controlling the Distribution of Supported Nanoparticles by Aqueous Synthesis," *Chemistry of Materials*, vol. 25, pp. 890-896, 2013.
- [38] J. Sietsma, J. Meeldijk, J. d. Breejen, M. Versluijs-Helder, A. v. Dillen, P. d. Jongh and K. d. Jong, "The Preparation of Supported NiO and Co₃O₄ Nanoparticles by the Nitric Oxide Controlled Thermal Decomposition of Nitrates," *Angewandte Chemie*, vol. 46, pp. 4547-4549, 2007.
- [39] M. Wolters, L. v. Grotel, T. Eggenhuisen, J. Sietsma, K. d. Jong and P. d. Jongh, "Combining confinement and NO calcination to arrive at highly dispersed supported nickel and cobalt oxide catalysts with a tunable particle size," *Catalysis Today*, vol. 163, pp. 27-32, 2011.
- [40] C. Liu, R. Liu, Y. Wu, Y. Wie and B. Fang, "Study on Electrochemical Properties of Palladium in Nitric Acid Medium," *Energy Procedia*, vol. 39, pp. 398-295, 2013.
- [41] N. Mahata and V. Vishwanathan, "Influence of Palladium Precursors on Structural Properties and Phenol Hydrogenation Characteristics of Supported Palladium Catalysts," *Journal of Catalysis*, vol. 196, pp. 262-270, 2000.
- [42] J. Sakauchi, H. Skagami, N. Takahasi, T. Matsuda and Y. Imizu, "Comparison of dinitrodiamminepalladium with palladium nitrate as a precursor for Pd/SiO₂ with respect to catalytic

- behavior for ethane hydroformylation and carbon monoxide hydrogenation," *Catalysis Letters*, vol. 99, no. 3-4, pp. 257-261, 2005.
- [43] S. Ali and J. Goodwin, "SSITKA Investigation of Palladium Precursor and Support Effects on CO Hydrogenation over Supported Pd Catalysts," *Journal of catalysis*, vol. 176, pp. 3-13, 1998.
- [44] M. Jayakumar, K. Venkatesan, T. Srinivasan and P. V. Rao, "Studies on the feasibility of electrochemical recovery of palladium from high-level liquid waste," *Electrochimica Acta*, vol. 54, pp. 1083-1088, 2009.
- [45] S. Tan and M. Piri, "Modeling the Solubility of Nitrogen Dioxide in Water Using Perturbed-Chain Statistical Associating Fluid Theory," *Industrial and Engineering Chemistry Research*, vol. 52, pp. 16032-16043, 2013.
- [46] C. Robertson, D. Mason and W. Corcoran, "Solubility of Oxygen in Nitric Acid mixtures," *Industrial and Engineering Chemistry*, pp. 1470-1472, 1955.
- [47] R. Svensson and E. Ljungstrom, "A kinetic study of the decomposition of HNO₃ and its reaction with NO," *International Journal of Chemical Kinetics*, vol. 20, no. 11, pp. 857-866, 1988.
- [48] C. Spicer, "Pubmed," 1993. [Online]. Available: <https://www.shivajicollege.ac.in/sPanel/uploads/econtent/3935dca57ebca74f279c0bf203678b2f.pdf>. [Accessed August 2021].
- [49] W. Mantële and E. Deniz, "UV–VIS absorption spectroscopy: Lambert-Beer reloaded," *Elsevier*, pp. 1386-1425, 2016.
- [50] S. Watanabe, a. T. Sato, T. Yoshida, M. Nakaya, M. Yoshino, T. Nagasaki, Y. Inaba, K. Takeshita and J. Onoe, "Spectroscopic and first-principles calculation studies of the chemical forms of palladium ion in nitric acid solution for development of disposal of high-level radioactive nuclear wastes," *AIP ADVANCES*, vol. 8, p. 045221, 2018.
- [51] W. Guan, S. Yamabe and S. Sakaki, "Interest in new heterodinuclear transition-metal/main-group-metal complexes: DFT study of electronic structure and mechanism of fluoride sensing function," *Dalton Trans.*, vol. 42, pp. 8717-8728, 2013.
- [52] S. Liu, E. Liu, Y. Wu, Y. Wei and B. Fang, "Study on Electrochemical Properties of Palladium in Nitric Acid Medium," *Energy Porcedia*, vol. 39, pp. 387-395, 2013.

- [53] M. Triest and H. B. C. R. G. Bussière, "Why does the middle band in the absorption spectrum of Ni(H₂O)₆²⁺ have two maxima?," *Journal of Chemical Education Internet*, 2000.
- [54] Q. M. Salman, "Spectroscopic study of UV-VIS electronic transitions of Ni²⁺ ions in different phases of Sol- Gel process," *Journal University of Kerbala*, pp. Vol. 14 No.4 34-43, 2016 .
- [55] N. Martin, P. Velin, M. Skoglundh, M. Bauer and P. Carlsson, "Catalytic hydrogenation of CO₂ to methane over supported Pd, Rh and Ni catalysts," *Catalysis Science and Technology*, vol. 7, pp. 1086-1094, 2017.
- [56] NileRed, "Making fuming nitric acid," https://www.youtube.com/watch?v=QmCdrDLyNXQ&t=279s&ab_channel=NileRed, 2018.
- [57] 曾刚, "A kind of preparation method of palladium nitrate". China Patent CN109592722A, 09 April 2019.
- [58] Handymath.com, "The Complete Aqueous Nitric Acid Solutions Density-Concentration Calculator," Handymath.com Solutions For Technicians, [Online]. Available: <https://www.handymath.com/cgi-bin/nitricble2.cgi?submit=Entry>. [Accessed May 2021].
- [59] B. Vats, S. Kannan, M. Sundararajan, M. Kumar and M. Drew, "Synthesis, structural and theoretical studies of dithiodiglycolamide compounds of palladium(II)," *Dalton Transactions*, vol. 44, no. 26, pp. 11867-11876, 2015.
- [60] H. Chen, Y. Liu, S. Peng and a. S. Liu, "New Bulky Phosphino-Pyridine Ligands. Palladium and Nickel Complexes for the Catalytic Polymerization and Oligomerization of Ethylene," *Organometallics*, vol. 22, no. 24, pp. 4893-4899, 2003.
- [61] E. K. Dann, E. Gibson, R. Catlow, P. Collier, T. Erden, D. Gianolio, C. Hardacre, A. Kroner, A. Raj, A. Goguet and P. P. Wells, "Combined In Situ CAFS/DRIFTS Studies of the Evolution of Nanoparticle Structures from Molecular Precursors," *Chemistry of Materials*, vol. 29, pp. 7515-7523, 2017.
- [62] S. Singh and P. Tandon, "Catalysis: A Brief Review on Nano-Catalyst," *Journal of Energy and Chemical Engineering*, vol. 2, pp. 106-115, 2014.
- [63] A. Venediktov, S. Korenev, S. Khranenko, S. Tkachev, P. Plyusnin, S. Mamonov and L. I. a. V. Vostrikov, "Properties of Nitric Acid Palladium Solutions with a High Metal Concentration," *Russian Journal of Applied Chemistry*, vol. 80, no. 5, pp. 695-704, 2007.

- [64] A. Krolak, I. Witonska, N. Krawczyk, M. Frajtak and S. Karski, "STABILITY OF Pd/SiO₂ AND Pd-Tl/SiO₂ CATALYSTS IN HYDRODECHLORINATION OF 2,4-DICHLOROPHENOL," *Revue Roumaine de Chimie*, vol. 56, no. 6, pp. 625-630, 2011.
- [65] S. Sitthisa, T. Pham, T. Prasomsri, T. Sooknoi, R. Mallinson and D. Resasco, "Conversion of furfural and 2-methylpentanal on Pd/SiO₂ and Pd-Cu/SiO₂," *Journal of Catalysis*, vol. 280, pp. 17-27, 2011.
- [66] A. Gutierrez, R. Kaila, M. Honkela, R. Slioor and A. Krause, "Hydrodeoxygenation of guaiacol on noble metal catalysts," *Catalysis Today*, vol. 147, pp. 239-245, 2009.
- [67] S. Sitthisa and D. Resasco, "Hydrodeoxygenation of Furfural Over Supported Metal Catalysts: A Comparative Study of Cu, Pd and Ni," *Catalysis Letters*, vol. 141, pp. 784-791, 2011.
- [68] A. Jongorius, R. Gosselink, J. Dijkstra, J. Bitter, P. Bruijninx and B. Weckhuysen, "Carbon nanofiber Supported Transition-Metal Carbide Catalysts for the Hydrodeoxygenation of Guaiacol," *Chemical Catalysis Chemistry*, vol. 5, pp. 2964-2972, 2013.
- [69] Q. Lai, C. Zhang and J. Holles, "Hydrodeoxygenation of guaiacol over Ni@Pd and Ni@Pt bimetallic overlayer catalysts," *Applied Catalysis A: General*, vol. 528, pp. 1-13, 2016.

9. Appendix

Table A1. XRD information of PdO and Pd(NO₃)₂·2H₂O from PDF data bank

Data	PdO 00-041-1107	Pd(NO ₃) ₂ (H ₂ O) ₂ 04-015-1243
#Copyright 2021 International Centre for Diffraction Data. All rights reserved.		
Creation date	19-5-2021	19-5-2021
Creation method	Generated by PDF-4+ 2020 4.20.0.1	
Chemical name	Palladium Oxide	Palladium Nitrate Hydrate
Chemical formula	Pd O	Pd (N O ₃) ₂ (H ₂ O) ₂
Chemical formula sum	O Pd	H4 N2 O8 Pd
Chemical formula weight	122.4	266.46
Cell length a	3.042(1)	4.9973(7)
Cell length b	3.042(1)	10.5982(14)
Cell length c	5.351(3)	11.7008(17)
Cell angle alpha	90	90
Cell angle beta	90	90
Cell angle gamma	90	90
Cell volume	49.52	619.7
Cell formula units Z	2	4
Symmetry cell setting	tetragonal	orthorhombic
Symmetry space group name H-M	P42/mmc	Pbca
Symmetry Int Tables number	131	61
Symmetry	1 x,y,z 2 -x,-y,-z 3 -x,-y,z 4 x,y,-z 5 -y,x,z+1/2 6 y,-x,-z+1/2 7 y,-x,z+1/2 8 -y,x,-z+1/2 9 -x,y,-z 10 x,-y,z 11 x,-y,-z 12 -x,y,z 13 y,x,-z+1/2 14 -y,-x,z+1/2 15 -y,-x,-z+1/2 16 y,x,z+1/2 14 -y,-x,z+1/2 15 -y,-x,-z+1/2 16 y,x,z+1/2	1 x,y,z 2 -x,-y,-z 3 x+1/2,-y+1/2,-z 4 -x+1/2,y+1/2,z 5 -x,y+1/2,-z+1/2 6 x,-y+1/2,z+1/2 7 -x+1/2,-y,z+1/2 8 x+1/2,y,-z+1/2

Figure A1. XRD spectrum of Pd(NO₃)₂·2H₂O, 04-015-1243.

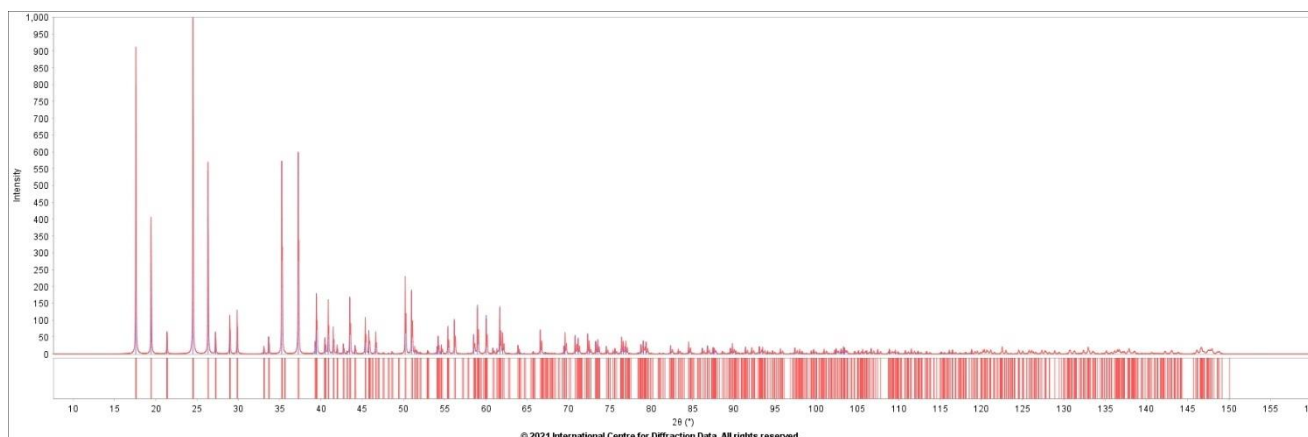


Figure A2. XRD spectrum of PdO, 00-041-1107.

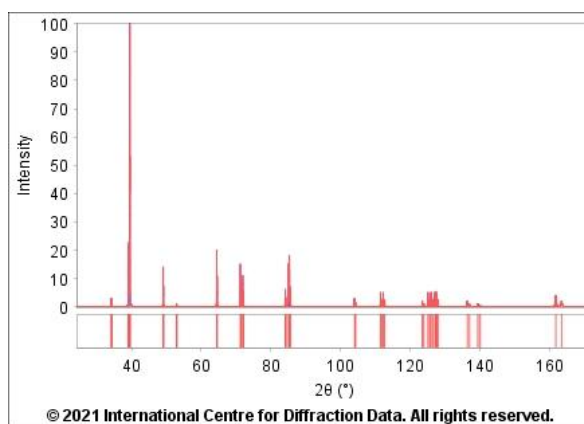


Figure A3. XRD spectrum of Pd, 00-005-0681.

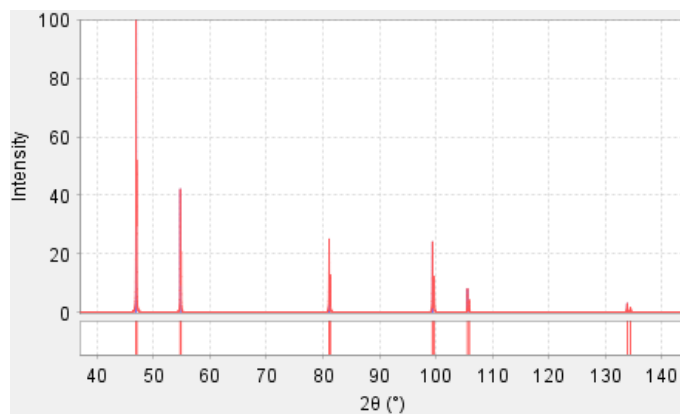


Figure A3. Certificate of Analysis for Pd(NO₃)₂·xH₂O from Sigma-Aldrich

SIGMA-ALDRICH[®] sigma-aldrich.com

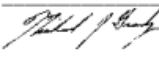
3050 Spruce Street, Saint Louis, MO 63103, USA
 Website: www.sigmaaldrich.com
 Email USA: techserv@sial.com
 Outside USA: eurtechserv@sial.com

Certificate of Analysis

Product Name: Palladium(II) nitrate hydrate

Product Number: **205761** Pd(NO₃)₂ · xH₂O
 Batch Number: **MKCL0231**
 Brand: ALDRICH
 CAS Number: 207596-32-5
 MDL Number: MFCD00149818
 Formula: N2O6Pd · xH2O
 Formula Weight: 230.43 g/mol
 Quality Release Date: 25 SEP 2019

Test	Specification	Result
Appearance (Color) Very Dark Brown	Conforms to Requirements	Very Dark Brown
Appearance (Form) Moist Powder and/or Chunks	Conforms to Requirements	Powder with Chunk(s)
X-Ray Diffraction Palladium (Pd)	Conforms to Structure 37.0 - 42.0 %	Conforms 39.1 %


 Michael Grady, Manager
 Quality Control
 Milwaukee, WI US

(a) 39.1% Palladium

SIGMA-ALDRICH[®] sigma-aldrich.com

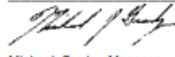
3050 Spruce Street, Saint Louis, MO 63103, USA
 Website: www.sigmaaldrich.com
 Email USA: techserv@sial.com
 Outside USA: eurtechserv@sial.com

Certificate of Analysis

Product Name: Palladium(II) nitrate hydrate

Product Number: **205761** Pd(NO₃)₂ · xH₂O
 Batch Number: **MKCM4344**
 Brand: ALDRICH
 CAS Number: 207596-32-5
 MDL Number: MFCD00149818
 Formula: N2O6Pd · xH2O
 Formula Weight: 230.43 g/mol
 Quality Release Date: 29 APR 2020

Test	Specification	Result
Appearance (Color) Very Dark Brown	Conforms to Requirements	Dark Brown
Appearance (Form) Moist Powder and/or Chunks	Conforms to Requirements	Powder with Chunk(s)
X-Ray Diffraction Palladium (Pd)	Conforms to Structure 37.0 - 42.0 %	Conforms 41.0 %


 Michael Grady, Manager
 Quality Control
 Milwaukee, WI US

(b) 41.0% Palladium